

Graphene quantum dots for valley-based quantum computing: A feasibility studyG. Y. Wu,^{1,2,*} N.-Y. Lue,¹ and L. Chang¹¹*Department of Physics, National Tsing-Hua University, Hsin-Chu 30013, Taiwan, Republic of China*²*Department of Electrical Engineering, National Tsing-Hua University, Hsin-Chu 30013, Taiwan, Republic of China*

(Received 31 October 2011; published 28 November 2011)

The rise of graphene opens a door to qubit implementation, as discussed in the recent proposal of valley pair qubits in double quantum dots of gapped graphene (G. Y. Wu, N.-Y. Lue, and L. Chang, [arXiv:1104.0443](https://arxiv.org/abs/1104.0443)). The work here presents the comprehensive theory underlying the proposal. It discusses the interaction of electrons with external magnetic and electric fields in such structures. Specifically, it examines a strong, unique mechanism, i.e., the analog of the first-order relativistic effect in gapped graphene. This mechanism is state mixing free and allows, together with electrically tunable exchange coupling, a fast, all-electric manipulation of qubits via electric gates, in the time scale of ns. The work also looks into the issue of fault tolerance in a typical case, yielding at 10 K a long qubit coherence time [$\sim O(\text{ms})$].

DOI: [10.1103/PhysRevB.84.195463](https://doi.org/10.1103/PhysRevB.84.195463)

PACS number(s): 73.63.Kv, 71.70.Ej, 68.65.Pq, 76.20.+q

I. INTRODUCTION

At the basis of quantum computing¹ realization is the physical implementation of qubits—two-state quantum information units. The rise of graphene^{2,3} has expanded the spectrum of materials suited to implementation. Graphene is a two-dimensional material with a unique electron dispersion, simulating that of Dirac particles. Because the dispersion has two degenerate, independent energy valleys, a degree of freedom (DOF)—the valley state of an electron—appears as a potential information carrier.⁴ This opens a path with distinctive advantages to encode quantum information—using “valley-based” qubits in quantum dots (QDs), as discussed in a recent proposal on valley pair qubits.⁵ The feasibility of valley qubits in graphene rings⁶ or valley control in other allotropes of carbon, e.g., carbon nanotube (CNT) QDs with disorder,⁷ have also been discussed recently and are based on different implementations and physical mechanisms.

Valley pair qubits utilize “valley singlet/triplet states” in double quantum dot (DQD) structures of gapped graphene to represent the logic 0/1 states, respectively. Notably, they are characterized by (a) scalability and fault tolerance, (b) all-electric manipulation via electric gates, and (c) a long coherence time, all being rather useful assets in qubit implementation. The principles underlying the qubits overlap with those developed for spin qubits, but with important differences.

In the spin case, for instance, the quantum dot (QD) approach (using confined electron spins)⁸ usually serves as the basis. Because of energy quantization, electron state coherence in QDs is generally enhanced. In addition, the exchange coupling between electrons in adjacent QDs is electrically tunable, aiding greatly the realization of all-electric qubit/qugate manipulation. Using the QD approach, various paradigm tactics may additionally be applied, including utilization of spin pair qubits to attain scalability and fault tolerance,^{9–13} the Rashba mechanism of spin-orbit interaction (SOI) to achieve coherent, electric manipulation of a single spin,^{14–16} and materials with weak SOI and vanishing hyperfine field (HF), such as graphene¹⁷ or CNT,¹⁸ in order to resolve the problem of state relaxation/decoherence.

The QD approach and the aforementioned tactics together constitute a good framework for the development of analogous qubits. However, being solutions to separate issues, the various tactics are sometimes at odds with one another in a material-dependent way. For instance, where a strong Rashba mechanism is available, the HF or the SOI inevitably cause state relaxation/decoherence,^{19–23} whereas in materials with weak SOI, qubit manipulation based on the mechanism of electron spin resonance is often employed or suggested^{24,25} which involves an ac magnetic field. For this reason, varied materials, e.g., GaAs,^{13,25,26} CNT,¹⁸ or InAs,²⁷ have been exploited, each suited to certain tactics, in the recent demonstration of spin qubits.

Interestingly, in the case of valley pair qubits in DQD structures of gapped graphene, these tactics can all be realized (in their “valley” version) without contradicting one another, thus providing a prospect for valley-based quantum computing.⁵ Graphene is a carbon allotrope and is therefore weak in both HF and SOI, giving rise to long spin coherence time.¹⁷ The qubit manipulation here is based on a unique mechanism, namely, the analog of the first-order relativistic effect due to the Dirac spectrum in gapped graphene. Being of “relativistic” origin, the mechanism is similar to the SOI, with strength comparable to that of the SOI in InAs. But there is a remarkable difference—it is valley-diagonal and hence state-mixing free, as opposed to the SOI. Based on the mechanism, a dc or ac electric field can be applied to modulate the orbital magnetic moment of a confined electron, creating a magnetic moment gradient in the DQD structure. In the presence of a static, uniform magnetic field, it results in a coherent qubit state rotation (in the effective Bloch sphere). For manipulation of the qubit into an arbitrary state, another rotation independent of the foregoing one is required, and is provided by exploiting the exchange coupling in the qubit. With these two rotations together, a fast, all-electric qubit manipulation may be performed by standard electric gate operation, in the time scale $\sim O(\text{ns})$. In a typical case, the valley relaxation time is estimated to be $O(\text{ms})$, sufficiently long for the manipulation.

This paper presents the comprehensive theory underlying valley pair qubits. The tuning of magnetic moment is one focus of this paper. It is discussed within a Schrodinger-

type equation including the first-order “relativistic correction” (R.C.). In addition, this paper examines the issue of qubit coherence and investigates specifically the phonon-mediated valley singlet-triplet transition. The presentation is organized as follows. Section II presents an overview of the principles underlying valley pair qubits. Sections III–VI supply the details. In particular, Sec. III provides the quantum-mechanical description of graphene QDs, including the Schrodinger-type equation with the “first-order R.C.” Section IV estimates the exchange interaction between two separately confined electrons in the DQD structure. Section V discusses the valley splitting in a QD, in the presence of a normal uniform magnetic field, and also derives the associated valley magnetic moment (μ_v) correct to the first-order R.C. In Sec. VI, μ_v tuning in dc and ac modes is discussed in relation to the qubit manipulation. Section VII investigates the phonon-mediated valley relaxation and the valley singlet-triplet transition. Section VIII summarizes the study. Appendix A provides a brief derivation of the Schrödinger-type equation for electrons in gapped graphene. Appendix B presents an alternative treatment of the ac electric effect on μ_v .

II. THE VALLEY PAIR QUBIT

A single-layer graphene is a gapless, two-dimensional material of hexagonal lattice structure, with a diatomic basis of carbon atoms. The electron energy dispersion simulates that of massless Dirac particles, with $E = \pm v_F |\mathbf{p}|$ (+ for the conduction band and – for the valence band), and the conduction and the valence bands touch at two Dirac points located at K and K' , respectively, of the Brillouin zone.^{2,3} Here v_F is the Fermi velocity. The corresponding energy valleys at K and K' are labeled by the isospin index τ_v ($\tau_v = 1$ for K and $\tau_v = -1$ for K') throughout the paper.

The implementation of valley qubits requires the presence of a gap between the conduction and the valence bands. Such a gap may be opened in a graphene layer epitaxially grown on a SiC or BN substrate, due to the substrate-induced asymmetry between the two basis atoms of a unit cell.^{28,29} The gap opening can be understood from the symmetry point of view as follows. In the gapless case, the fact that conduction and valence bands are degenerate at the Dirac points is tied to the inversion symmetry in graphene. The substrates SiC or BN lack the symmetry and hence break the symmetry in graphene, resulting in the opening of a gap. Since the gap opening is also an important target for the researchers interested in building up semiconducting graphene-based electronics, we are optimistic that, with the present intensive efforts in this area, technologies will be developed for routine growth of gapped graphene.

In gapped graphene, the corresponding electron dispersion $E = \pm(\Delta^2 + v_F^2 p^2)^{1/2}$ (+for the conduction band, and –for the valence band) is characterized by the energy gap 2Δ and the effective mass $m^* = \Delta/v_F^2$. QDs may be formed via electrostatic modulation of the energy bands in space, where the energy gap is utilized to confine electrons or holes. In the paper, we shall focus on electrons. (The discussion applies to holes as well.)

Figure 1 shows the valley qubit system—a DQD structure defined electrostatically, for example, by back gates (not shown here). Gate V_C tunes the potential barrier between the QDs and

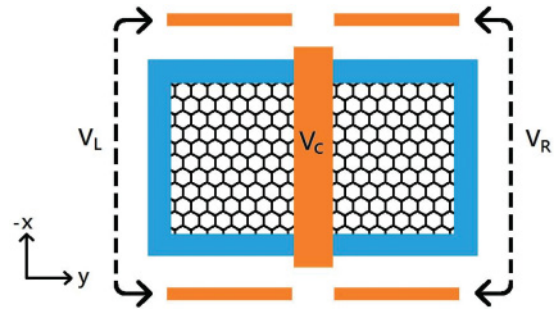


FIG. 1. (Color online) The DQD qubit structure. The QDs are electrostatically defined, for example, by back gates (not shown in the figure). Gate V_C is used to tune the potential barrier. Gates V_L and V_R are applied for dc and ac μ_v tuning.

hence the corresponding interdot tunneling. Gates V_L and V_R are applied to produce dc and ac electric fields across the QDs, for tuning of electron magnetic moments in the QDs, as discussed later.

In the absence of magnetic field, each QD is assumed to accommodate only one quantized energy level. The level is fourfold degenerate, consisting of the quadplet $|\tau_v = \pm 1, \sigma = \pm 1/2\rangle$ (one-electron states), in association with the valley (τ_v) and the spin (σ) degeneracy. The qubit implementation requires placement of the structure in a tilted, uniform magnetic field, denoted as B_{total} ($\mathbf{B}_{\text{total}} = \mathbf{B}_{\text{plane}} + \mathbf{B}_{\text{normal}}$). See Fig. 2. Here, B_{plane} is the in-plane component and B_{normal} is the component normal to the graphene layer of the magnetic field. The presence of a tilted magnetic field serves multiple purposes. It removes the redundant spin DOF in the implementation of valley qubits as well as provides the “Larmor precession” of qubits, as shall become clear below.

The magnetic field couples to both the spin and valley DOFs of an electron, according to the following Zeeman-type interaction:

$$H_Z = -g^* s \mu_B |B_{\text{total}}| + \tau_v \mu_v |B_{\text{normal}}|. \quad (2.1)$$

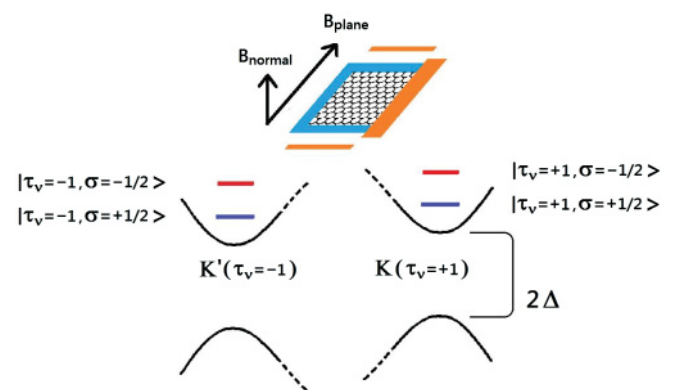


FIG. 2. (Color online) One-electron energy levels in a QD placed in the tilted magnetic field B_{total} ($\mathbf{B}_{\text{total}} = \mathbf{B}_{\text{plane}} + \mathbf{B}_{\text{normal}}$). Conduction and valence bands of gapped graphene are also shown. The Zeeman-type interaction for spin and valley DOFs, $H_Z = -g^* \sigma \mu_B |B_{\text{total}}| + \tau_v \mu_v |B_{\text{normal}}|$, splits the quadplet $|\tau_v = \pm 1, \sigma = \pm 1/2\rangle$. For $g^* \mu_B |\sigma B_{\text{total}}| > \mu_v |B_{\text{normal}}|$, the splitting leaves $|\tau_v = \pm 1, \sigma = \pm 1/2\rangle$ as the lower valley doublet.

Here g^* is the electron g factor, μ_B is the Bohr magneton, and μ_v is the valley-dependent magnetic moment associated with the orbital motion of an electron in gapped graphene.³⁰ As expressed in the equation, B_{total} interacts with the spin DOF, giving the usual Zeeman energy $g^* \sigma \mu_B |B_{\text{total}}|$ and quantizing the spin in the direction of B_{total} , while B_{normal} couples additionally to the valley DOF, giving the corresponding ‘‘valley’’ Zeeman term $\tau_v \mu_v |B_{\text{normal}}|$. For $\frac{1}{2} g^* \mu_B |B_{\text{total}}| > \mu_v |B_{\text{normal}}|$, the spin splitting leaves $|\tau_v = \pm 1, \sigma = 1/2\rangle$ as the lower valley doublet in each QD. The notations $\{K_L, K'_L\}$ and $\{K_R, K'_R\}$ are used to denote the lower doublets confined in the left and right QDs, respectively. (The spin index is omitted, being fixed at $\sigma = 1/2$ here.) These constitute the basis set of one-electron states in forming qubit states, which are two-electron states, as explained next.

The valley pair qubit operates in the low-energy sector, with the corresponding charge configuration (1,1), meaning that the two electrons are separately confined in the QDs and occupy the one-electron states $\{K_L, K'_L\}/\{K_R, K'_R\}$. Virtual electron hopping between the QDs couples the (1,1) configuration to the configuration (0,2) (where the electrons both reside in the same QD), giving rise to the Heisenberg-type exchange interaction

$$H_J = \frac{1}{4} J \vec{\tau}_L \cdot \vec{\tau}_R, \quad J \sim 4t_{d-d}^2/U. \quad (2.2)$$

Here, J is the exchange coupling, t_{d-d} is the interdot tunneling, and U is the energy detuning of (0,2) from (1,1). J is tunable via gate V_C (which controls t_{d-d}) or back gates (which controls U). $\tau_{L(R)}$ is the Pauli valley operator, with

$$\tau_x = \begin{pmatrix} 0 & 1 \\ 1 & 0 \end{pmatrix}, \quad \tau_y = \begin{pmatrix} 0 & -i \\ i & 0 \end{pmatrix}, \quad \tau_z = \begin{pmatrix} 1 & 0 \\ 0 & -1 \end{pmatrix}.$$

The logic 0/1 states are represented by the eigenstates of H_J , i.e., the valley singlet $|z_S\rangle$ /triplet $|z_{T0}\rangle$. Here,

$$\begin{aligned} |z_S\rangle &= \frac{1}{\sqrt{2}} (c_{K_L}^+ c_{K'_R}^+ - c_{K'_L}^+ c_{K_R}^+) |\text{vacuum}\rangle, \\ |z_{T0}\rangle &= \frac{1}{\sqrt{2}} (c_{K_L}^+ c_{K'_R}^+ + c_{K'_L}^+ c_{K_R}^+) |\text{vacuum}\rangle, \end{aligned} \quad (2.3)$$

in terms of electron creation operators for the QD-confined states $\{K_L, K'_L, K_R, K'_R\}$. Linear combinations of $\{|z_S\rangle, |z_{T0}\rangle\}$ give

$$|x_+\rangle = c_{K_L}^+ c_{K'_R}^+ |\text{vacuum}\rangle, \quad |x_-\rangle = c_{K'_L}^+ c_{K_R}^+ |\text{vacuum}\rangle.$$

The qubit state space (denoted as Γ_v) is expanded by $|z_S\rangle$ and $|z_{T0}\rangle$, and isomorphic to the spin-1/2 state space, e.g., $|z_S\rangle \leftrightarrow |s_z = -1/2\rangle$, $|z_{T0}\rangle \leftrightarrow |s_z = 1/2\rangle$, $|x_-\rangle \leftrightarrow |s_x = -1/2\rangle$, $|x_+\rangle \leftrightarrow |s_x = 1/2\rangle$. The other triplet states,

$$|z_{T+}\rangle = c_{K_L}^+ c_{K'_R}^+ |\text{vacuum}\rangle, \quad |z_{T-}\rangle = c_{K'_L}^+ c_{K_R}^+ |\text{vacuum}\rangle,$$

are outside Γ_v and not needed for quantum computing.

Equations (2.1) and (2.2) determine the energy levels of various two-electron states. See Fig. 3. B_{normal} splits $|z_{T\pm}\rangle$ away from $\{|z_S\rangle, |z_{T0}\rangle\}$, by $(\mu_{vL} + \mu_{vR})|B_{\text{normal}}|$. $|z_S\rangle$ and $|z_{T0}\rangle$ are separated by J , while $|x_-\rangle$ and $|x_+\rangle$ by $2(\mu_{vL} - \mu_{vR})|B_{\text{normal}}|$. Here, μ_{vL} and μ_{vR} are the valley magnetic moments in the left and right QDs, respectively. Overall, the qubit system

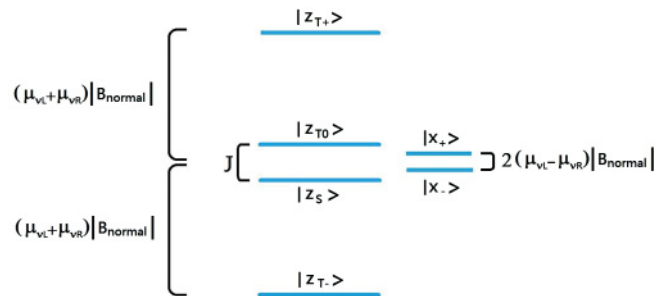


FIG. 3. (Color online) Two-electron energy levels in the DQD. $|z_{T\pm}\rangle$ are split away from $\{|z_S\rangle, |z_{T0}\rangle\}$, by $\pm(\mu_{vL} + \mu_{vR})|B_{\text{normal}}|$, respectively. $|z_S\rangle$ and $|z_{T0}\rangle$ are split in energy by J , while $|x_-\rangle$ and $|x_+\rangle$ by $2(\mu_{vL} - \mu_{vR})|B_{\text{normal}}|$.

is described by the following effective Hamiltonian in the reduced space Γ_v :

$$H_{\text{eff}} = (\mu_{vL} - \mu_{vR})B_{\text{normal}}\tau_x + \frac{J}{2}\tau_z \quad (2.4)$$

in the basis of $\{|z_S\rangle, |z_{T0}\rangle\}$.

H_{eff} governs the time evolution of the qubit state. The τ_x part generates a rotation $\hat{R}(\theta_x = \Omega_x t_x)$ about the x axis (of the Bloch sphere) when it is applied for the time t_x , where Ω_x is the Larmor frequency, e.g., $\Omega_x = 2(\mu_{vL} - \mu_{vR})B_{\text{normal}}/\hbar$. The τ_z part generates a rotation $\hat{R}_z(\theta_z = \Omega_z t_z)$ about the z axis ($\Omega_z = J/\hbar$, and t_z is the corresponding time). Together, \hat{R}_x and \hat{R}_z allow for the manipulation of a single qubit. See Fig. 4.

According to Eq. (2.4), a gradient in the magnetic moment, i.e., $\mu_{vL} \neq \mu_{vR}$, is a required condition for the manipulation. Because the magnetic moment is energy dependent, it can be modulated by tuning the electron energy level in the QD (as discussed in Sec. V). Therefore, a structural differentiation in the QDs may provide the required gradient. There are also controllable, electric means of modulating μ_{vL}/μ_{vR} in dc or ac modes via back gates or gates V_L/V_R in order to furnish the gradient (the latter being discussed in Sec. VI). In the dc mode, $(\mu_{vL} - \mu_{vR})$ is time independent, and an initial qubit state, e.g., $|\Phi(t=0)\rangle = |z_S\rangle$, undergoes the following rotation:

$$\begin{aligned} |\Phi(t)\rangle &= \hat{R}_n(\theta_n^{(\text{dc})})|z_S\rangle, \\ \hat{R}_n(\theta_n^{(\text{dc})}) &= \exp\left(-\frac{i}{2}\vec{\tau} \cdot \vec{\theta}_n^{(\text{dc})}\right), \\ \vec{\theta}_n^{(\text{dc})} &= \frac{t}{\hbar}(2(\mu_{vL} - \mu_{vR})B_{\text{normal}}, 0, J), \end{aligned} \quad (2.5)$$

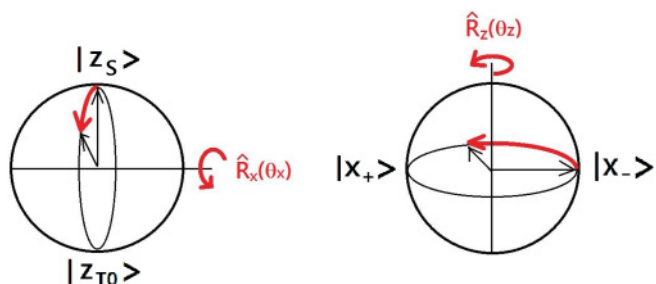


FIG. 4. (Color online) The time evolution of a qubit state, as governed by H_{eff} , consists of a rotation $\hat{R}_x(\theta_x)$ about the x axis of the Bloch sphere, and a rotation $\hat{R}_z(\theta_z)$ about the z axis. θ_x and θ_z are the respective angles of rotation.

where the direction and the magnitude of $\theta_n^{(\text{dc})}$ determine the axis and the angle of rotation, respectively. Tuning of the ratio $(\mu_{vL} - \mu_{vR}) : J$ by V_L , V_R , and V_C (or back gates) determines the direction of $\theta_n^{(\text{dc})}$, and tuning of the time length t determines the magnitude of $\theta_n^{(\text{dc})}$. On the other hand, the manipulation can also be performed in the ac mode, where $(\mu_{vL} - \mu_{vR})$ varies periodically in time, as discussed in Sec. VI. It allows the application of qubit resonance techniques to qubit manipulation, with the Rabi frequency $\Omega_R = \Omega_z$. Although the application has initially been suggested to be performed via periodic modulation of the exchange coupling J ,¹⁰ the alternative provided here—periodic modulation of $(\mu_{vL} - \mu_{vR})$ —adds another dimension to it.

This qubit implementation is the analog of the spin pair scheme.^{9–13} It shares the distinctive advantages provided in the scheme, e.g., scalability and fault tolerance, and the method developed in the scheme for the initialization-readout-qutate operation¹² may be adapted here. For example, the following electrical readout method is suggested. One can bias the two quantum dots asymmetrically in a qubit such that the (1,1) charge configuration (meaning one electron per quantum dot) is projected to the (0,2) configuration (meaning that both of the electrons now reside in the same quantum dot). The projection depends on the qubit state as follows. Because the (0,2) singlet and triplet states differ sizably in energy (with the difference being basically that between the ground state and the first excited state in the quantum dot), the bias asymmetry between the quantum dots can be set such that only the (1,1) singlet state can successfully make the transition to the (0,2) singlet, while the (1,1) triplet does not make the transition to the (0,2) triplet (i.e., a valley blockade phenomenon). After the projection, a quantum point contact sensor near one of the quantum dot is used to measure the charge number in the quantum dot. This provides the readout of the valley qubit state.

As Eq. (2.4) forms the basis of qubit manipulation, it constitutes the core of the discussion in Secs. III–VI. These sections supplement the argument leading to Eq. (2.4), estimate the parameters (e.g., μ_{vL} , μ_{vR} , and J) in the equation, discuss ways to control the parameters, and the qubit manipulation based on the equation.

III. THE QUANTUM MECHANICAL DESCRIPTION

It is obvious from Sec. II that tuning of the magnetic moment (μ_{vL} and μ_{vR}) is an important part of the qubit manipulation. In order to prepare the background for the discussion of tuning, this section describes the quantum mechanics of a graphene QD in the presence of both an in-plane electric field and a normal magnetic field B_{normal} .

An electron in the case satisfies the following Dirac-type equation:³

$$\begin{aligned} H_D \phi_D &= E \phi_D, \\ H_D &= H_0(\tau_v) + H_{\text{electric}} + H_{\text{magnetic}}(\tau_v), \\ \phi_D &= \begin{pmatrix} \phi_A \\ \phi_B \end{pmatrix}, \\ H_0(\tau_v) &= \begin{pmatrix} \Delta & v_F(\hat{p}_x - i\tau_v \hat{p}_y) \\ v_F(\hat{p}_x + i\tau_v \hat{p}_y) & -\Delta \end{pmatrix}, \end{aligned}$$

$$H_{\text{electric}} = \begin{pmatrix} V & 0 \\ 0 & V \end{pmatrix},$$

$$H_{\text{magnetic}}(\tau_v) = e v_F \begin{pmatrix} 0 & A_x - i\tau_v A_y \\ A_x + i\tau_v A_y & 0 \end{pmatrix},$$

$$V = V_{\text{QD}} + V_\varepsilon. \quad (3.1)$$

Here, H_D is the Dirac Hamiltonian, Φ_D is the two-component Dirac wave function, V_{QD} is the confining QD potential energy, V_ε is the external electric potential energy, and (A_x, A_y) is the vector potential in association with the magnetic field.

For the qubit implementation, we consider the case where $E \sim \Delta$ (the “nonrelativistic limit”). In this limit, Eq. (3.1) is reduced to the following Schrödinger-type equation [correct to $O(B_{\text{normal}})$ and the first-order R.C.]:

$$H\phi = E\phi, \quad H = H^{(0)} + H^{(1)}. \quad (3.2)$$

$H^{(0)}$ is the nonrelativistic part, with

$$H^{(0)} = \frac{\vec{\pi}^2}{2m^*} + V + \tau_v \mu_{v0} B_{\text{normal}},$$

and $H^{(1)}$ is the first-order R.C., with

$$\begin{aligned} H^{(1)} &= \tau_v \frac{\hbar}{4m^* \Delta} [(\nabla V) \times \vec{\pi}]_{\text{normal}} \quad (\text{VOI}) \\ &\quad - \frac{1}{2\Delta} \left(\frac{\vec{\pi}^2}{2m^*} + \tau_v \mu_{v0} B_{\text{normal}} \right)^2 - \frac{1}{8m^* \Delta} (\vec{p}^2 V), \\ \vec{\pi} &= \vec{p} + e\vec{A}, \quad \mu_{v0} = \frac{e\hbar}{2m^*}. \end{aligned}$$

H is the Schrödinger Hamiltonian, and Φ denotes the one-component Schrödinger wave function. The electron energy E is now defined with respect to the conduction-band edge. $H^{(0)}$ describes the motion of a charged particle in the magnetic field B_{normal} . The last term $\tau_v \mu_{v0} B_{\text{normal}}$ in $H^{(0)}$ gives rise to the valley splitting in the field, with $\mu_{v0} = e/2m^*$ being the nonrelativistic valley magnetic moment, the analog of the Bohr spin magneton. The first term in $H^{(1)}$ is called the valley-orbit interaction (VOI),³¹ the analog of spin-orbit interaction. The second term is the usual first-order relativistic correction to the nonrelativistic kinetic energy. The third term is the Darwin’s term. Equation (3.2) is derived in Appendix A. Equations (3.1) and (3.2) shall be utilized in Sec. V.

The appearance of VOI can be roughly understood as follows, if we choose to describe physics in the reference frame which moves with the electron. In the presence of the electric field ∇V in the laboratory reference frame, the transformation of electromagnetic fields introduces an effective magnetic field proportional to $[(\nabla V) \times \vec{\pi}]_{\text{normal}}$ in the moving frame. The interaction between the effective magnetic field and the valley magnetic moment gives rise to the VOI.

IV. THE EXCHANGE COUPLING J

The tuning of the exchange coupling constitutes an important part of qubit manipulation in the quantum dot approach.^{8,10–13} This is also true in the case of valley pair qubits. In this section, the coupling is evaluated for near-gap electrons (i.e., the nonrelativistic limit). We consider the double graphene QDs (with size $\sim L$), as shown in Fig. 1,

and estimate J using the formula

$$J \sim 4t_{d-d}^2/U. \quad (4.1)$$

We assume that the two QDs are identical, and there is only one confined level in each QD, with energy E (relative to the conduction-band edge). U here reduces to the on-site Coulomb energy. The depth of the QD potential is denoted as V_0 and taken to be of the order of E . Specifically, we use $V_0 = 2E$. In the nonrelativistic limit, where the Schrödinger-type equation (3.2) applies, we estimate roughly

$$t_{d-d} \sim O(1)E \exp(-2\alpha W), \quad \alpha = \frac{\sqrt{2m^*(V_0 - E)}}{\hbar}. \quad (4.2)$$

Here, W is the interdot potential barrier width. Using $\Delta \sim 0.14$ eV,²⁸ $v_F = 10^6$ m/s, $L \sim 350$ Å, $E \sim 30$ meV, $U \sim 10$ meV, and $W \sim 0.5 L$ in Eqs. (4.1) and (4.2), we obtain $J \sim O(1)$ meV. Lower values of J can be obtained by increasing W , the interdot barrier height (via gate V_C), or the detuning U (via back gates).^{12,13}

V. THE VALLEY SPLITTING AND THE VALLEY MAGNETIC MOMENT IN A QD

This section discusses the valley splitting in a QD, in the presence of a normal magnetic field B_{normal} , as well as the valley magnetic moment μ_v . The result shall be utilized in the discussion of magnetic moment tuning in Sec. VI. Throughout the paper, we assume the weak magnetic field limit, e.g.,

$$l_{\text{orbital}} \ll l_B, \quad l_{\text{orbital}} \sim L, \quad l_B = \sqrt{\frac{\hbar}{eB_{\text{normal}}}}.$$

l_{orbital} is the electron orbital size, L is the QD size, and l_B is the magnetic length. We shall neglect the terms which are $O(B_{\text{normal}}^2)$ in the calculation. Moreover, in the regime considered here, QD size confinement dominates over Landau-level quantization, allowing for the discussion of magnetic effects here to be carried out within the perturbation theory.

A general discussion of valley splitting is given first, based on the Dirac equation (3.1).³² We begin with the case of gapless graphene, i.e., $\Delta = 0$. It is straightforward to verify that if (Φ_A, Φ_B) is a solution to Eq. (3.1) for $\tau_v = 1$, then in association with it, there is a degenerate solution (Φ_B, Φ_A) , with $\tau_v = -1$. Therefore, in order to produce a valley splitting, the condition $\Delta \neq 0$ is required. We turn to the case of gapped graphene below.

The valley splitting in the case is analyzed in the framework of perturbation theory. Again, Eq. (3.1) is utilized for a general discussion first. For $B_{\text{normal}} = 0$, H_{magnetic} vanishes and Eq. (3.1) reduces to

$$[H_0(\tau_v) + H_{\text{electric}}] \phi_D^{(0)}(\tau_v) = E^{(0)} \phi_D^{(0)}(\tau_v). \quad (5.1)$$

Owing to time-reversal symmetry, the states for $\tau_v = \pm 1$ are degenerate. Specifically, one can verify that if $(\Phi_A^{(0)}, \Phi_B^{(0)})$ is a solution to Eq. (5.1) for $\tau_v = 1$, then $(-\Phi_B^{(0)*}, \Phi_A^{(0)*})$ is a solution with the same energy, for $\tau_v = -1$, i.e.,

$$\begin{aligned} & [\phi_A^{(0)}(x, y; \tau_v), \phi_B^{(0)}(x, y; \tau_v)] \\ &= [-\phi_B^{(0)*}(x, y; -\tau_v), \phi_A^{(0)*}(x, y; -\tau_v)]. \end{aligned} \quad (5.2)$$

For $B_{\text{normal}} \neq 0$, we treat H_{magnetic} as a perturbation. [We choose the asymmetric gauge $(A_x, A_y) = (0, B_{\text{normal}}x)$ to simplify the discussion here.] It gives the following first-order energy correction (linear in B_{normal})

$$\begin{aligned} E_Z(\tau_v) &= \langle \phi_D^{(0)}(\tau_v) | H_{\text{magnetic}}(\tau_v) | \phi_D^{(0)}(\tau_v) \rangle \\ &= 2ev_F \tau_v \text{Imag}[\langle \phi_A^{(0)}(\tau_v) | A_y | \phi_B^{(0)}(\tau_v) \rangle]. \end{aligned} \quad (5.3)$$

Using Eq. (5.2), one can show that $\text{Imag}[\langle \phi_A^{(0)}(\tau_v) | A_y | \phi_B^{(0)}(\tau_v) \rangle]$ here is actually τ_v independent. Thereby, $E_Z(\tau_v) \propto \tau_v$, carrying opposite signs for the $\tau_v = \pm 1$ states and showing Zeeman valley splitting. Moreover, the splitting size is generally QD structure dependent, as it depends on the wave function of the quantized state.

Now, we proceed to a more detailed discussion of valley splitting, based on the Schrödinger-type equation (3.2). We consider specifically a rectangular QD, and write [correct to $O(B_{\text{normal}})$]

$$\begin{aligned} H &\simeq H_{B\tau}^{(0)} + H_{B0}^{(0)} + H_{0\tau}^{(1)} + H_{B\tau}^{(1)} + H_{\text{rest}}, \\ H_{B\tau}^{(0)} &= \frac{\vec{p}^2}{2m^*} + V + \tau_v \mu_{v0} B_{\text{normal}}, \quad H_{B0}^{(0)} = \frac{e\vec{A} \cdot \vec{p}}{m^*}, \\ H_{0\tau}^{(1)} &= \tau_v \frac{\hbar}{4m^* \Delta} [(\nabla V) \times \vec{p}]_{\text{normal}}, \\ H_{B\tau}^{(1)} &= -\tau_v \mu_{v0} \left(B_{\text{normal}} \frac{\vec{p}^2}{2m^* \Delta} + \frac{1}{2\Delta} [\vec{A} \times (\nabla V)]_{\text{normal}} \right). \end{aligned} \quad (5.4)$$

Here, $V = V_{\text{QD}} = \frac{1}{2}m^*(w_x^2 + w_y^2)$ (for a rectangular QD), with $O(w_x) \sim O(w_y)$. H has been expressed in a form convenient for the perturbative calculation. Each term in H is labeled with two subscripts, with the first one (B or 0) denoting whether it is B_{normal} dependent, and the second one (τ or 0) denoting whether it is τ_v dependent. $H_{B\tau}^{(0)}$ describes a two-dimensional (2D) anisotropic simple harmonic oscillator with valley splitting. The corresponding oscillator function is denoted as $\Phi_{nm}^{(0)}$ [(n, m) being the 2D harmonic oscillator indices]. The other terms in Eq. (5.4) are treated as the perturbation. These terms (except H_{rest}) lead to the energy correction linear in both B_{normal} and τ_v (i.e., the Zeeman energy E_Z). H_{rest} is both τ_v and B_{normal} independent, and irrelevant for the calculation of valley splitting.

The perturbation theory gives the following Zeeman energy and valley magnetic moment:

$$\begin{aligned} E_Z(\tau_v) &\approx \tau_v \mu_{v0} B_{\text{normal}} + \langle \phi_{00}^{(0)} | H_{B\tau}^{(1)} | \phi_{00}^{(0)} \rangle \\ &+ 2 \text{Real} \left[\langle \phi_{00}^{(0)} | H_{B0}^{(0)} | \phi_{11}^{(0)} \rangle \frac{1}{\hbar(-w_x - w_y)} \right. \\ &\quad \left. \times \langle \phi_{11}^{(0)} | H_{0\tau}^{(1)} | \phi_{00}^{(0)} \rangle \right] \\ &= \tau_v \mu_v B_{\text{normal}}, \\ \mu_v &= \mu_{v0} \left[1 - \frac{\hbar}{2\Delta} \frac{w_x w_y}{(w_x + w_y)} \right]. \end{aligned} \quad (5.5)$$

The second term in μ_v derives from the first-order R.C.

VI. μ_v TUNING IN dc AND ac MODES AND QUBIT MANIPULATION

As Eq. (5.5) shows, μ_v depends on w_x and w_y —parameters in the QD potential V_{QD} . It suggests a way to tune μ_v via

modulation of the potential. Below, we investigate electric means of the modulation, in either dc or ac modes.

First, we consider a QD in the presence of a dc uniform electric field ($\varepsilon_x^{(dc)}$ in the x direction) as well as the normal, uniform magnetic field B_{normal} , where V_{QD} consists of a dominant quadratic potential and a weak anharmonic one. Two cases are analyzed. In one case, the anharmonic term is cubic (x^3). In the other, it is quadric (x^4). The presence of the anharmonic term is required because, without it, the electric field would just shift the electron equilibrium position without altering the physics.

We consider the cubic case now. Let

$$V = V_{\text{QD}} + e\varepsilon_x^{(dc)}x, \quad V_{\text{QD}} = V_2 + V_3, \\ V_2 = \frac{1}{2}m^*w_0^2(x^2 + y^2), \quad V_3 = \frac{1}{3}k_{3x}m^*w_0^2x^3.$$

Here, k_{3x} characterizes the strength of V_3 . We assume that both k_{3x} and $\varepsilon_x^{(dc)}$ are weak [$k_{3x} \ll (m^*w_0/\hbar)^{1/2}$, $e\varepsilon_x^{(dc)} \ll (m^*w_0^3)^{1/2}$], and derive the effect of $\varepsilon_x^{(dc)}$ on the valley splitting. We introduce $x_\varepsilon^{(dc)} \equiv -e\varepsilon_x^{(dc)}/m^*w_0^2$, the shift in electron equilibrium position due to the electric field, and write

$$V \approx \frac{1}{2}m^*w_0^2[(x - x_\varepsilon^{(dc)})^2 + y^2] \\ + \frac{1}{3}k_{3x}m^*w_0^2(x - x_\varepsilon^{(dc)})^3 \\ + k_{3x}m^*w_0^2x_\varepsilon^{(dc)}(x - x_\varepsilon^{(dc)})^2, \\ \xrightarrow{x - x_\varepsilon^{(dc)} \rightarrow x} \frac{1}{2}m^*w_0^2(x^2 + y^2) + \frac{1}{3}k_{3x}m^*w_0^2x^3 \\ + k_{3x}m^*w_0^2x_\varepsilon^{(dc)}x^2,$$

correct up to $O(x_\varepsilon^{(dc)})$. Here, a change of coordinates $x - x_\varepsilon^{(dc)} \rightarrow x$ has been made. The above result shows that the dc field modifies the quadratic potential as follows:

$$\frac{1}{2}m^*w_0^2(x^2 + y^2) \rightarrow \frac{1}{2}m^*(w_x^2x^2 + w_0^2y^2), \\ w_x^2 = w_0^2(1 + 2k_{3x}x_\varepsilon^{(dc)}),$$

giving it a slight anisotropy. Using the result in Eq. (5.5) for a rectangular QD, we obtain the $\varepsilon_x^{(dc)}$ -induced Zeeman energy

$$\delta E_Z^{(dc)}(\tau_v) \approx -\frac{1}{8}\tau_v\mu_{v0}B_{\text{normal}}(k_{3x}x_\varepsilon^{(dc)})\frac{\hbar w_0}{\Delta}. \quad (6.1)$$

Correspondingly, it gives the $\varepsilon_x^{(dc)}$ -induced valley magnetic moment tuning

$$\delta\mu_v^{(dc)} \approx -\mu_{v0}\frac{1}{8}(k_{3x}x_\varepsilon^{(dc)})\frac{\hbar w_0}{\Delta}. \quad (6.2)$$

The results in Eqs. (6.1) and (6.2) both are linear in $\hbar w_0/\Delta$, the ratio of the ground-state energy to the ‘‘rest mass’’ energy, showing that these are the first-order relativistic effects.

Next, we consider the quadric case:

$$V = V_{\text{QD}} + e\varepsilon_x^{(dc)}x, \quad V_{\text{QD}} = V_2 + V_4, \\ V_2 = \frac{1}{2}m^*w_0^2(x^2 + y^2), \quad V_4 = \frac{1}{4}k_{4x}m^*w_0^2x^4.$$

Here, k_{4x} characterizes the strength of V_4 . Note that the energy eigenvalue in this case is an even function, i.e., $E(\tau_v; \varepsilon_x^{(dc)}) = E(\tau_v; -\varepsilon_x^{(dc)})$. [It can be shown that if $\Phi(x, y; \tau_v)$ is an eigenstate (in the field $\varepsilon_x^{(dc)}$) with the energy $E(\tau_v; \varepsilon_x^{(dc)})$, then $\Phi^*(-x, y; \tau_v)$ is a solution (in the field $-\varepsilon_x^{(dc)}$) with the

same energy.] This result is used below. We also note that $V_2 + V_4$ with $k_{4x} < 0$ describes a parabolic confining potential with a cutoff in the x direction. (One can also add a similar y^4 term to cut off the potential in the y direction, without affecting the discussion in this section.) Therefore, the presence of V_4 is a realistic assumption.

We assume that both k_{4x} and $\varepsilon_x^{(dc)}$ are weak [$k_{4x} \ll m^*w_0/\hbar$, $e\varepsilon_x^{(dc)} \ll (\hbar m^*w_0^3)^{1/2}$], and derive the effect of $\varepsilon_x^{(dc)}$ on the valley splitting. We write

$$V \approx \frac{1}{2}m^*w_0^2[(x - x_\varepsilon^{(dc)})^2 + y^2] \\ + \frac{1}{4}k_{4x}m^*w_0^2(x - x_\varepsilon^{(dc)})^4 \\ + k_{4x}m^*w_0^2x_\varepsilon^{(dc)}(x - x_\varepsilon^{(dc)})^3 \\ + \frac{3}{2}k_{4x}m^*w_0^2x_\varepsilon^{(dc)2}(x - x_\varepsilon^{(dc)})^2 \\ \xrightarrow{x - x_\varepsilon^{(dc)} \rightarrow x} \frac{1}{2}m^*w_0^2(x^2 + y^2) + \frac{1}{4}k_{4x}m^*w_0^2x^4 \\ + k_{4x}m^*w_0^2x_\varepsilon^{(dc)}x^3 + \frac{3}{2}k_{4x}m^*w_0^2x_\varepsilon^{(dc)2}x^2, \\ x_\varepsilon^{(dc)} = -e\varepsilon_x^{(dc)}/m^*w_0^2,$$

correct up to $O(x_\varepsilon^{(dc)2})$. We further drop the linear-in- $x_\varepsilon^{(dc)}$ cubic potential term $k_{4x}m^*w_0^2x_\varepsilon^{(dc)}x^3$ from V . Since $E(\tau_v; \varepsilon_x^{(dc)}) = E(\tau_v; -\varepsilon_x^{(dc)})$, the contribution of this term to the energy cannot be linear. Instead, it is $O(k_{4x}^2x_\varepsilon^{(dc)2})$ or of a higher order, which is negligible in comparison to the result that will be derived below. Thereby, we write

$$V \approx \frac{1}{2}m^*(w_x^2x^2 + w_0^2y^2) + \frac{1}{4}k_{4x}m^*w_0^2x^4, \\ w_x^2 = w_0^2(1 + 3k_{4x}x_\varepsilon^{(dc)2}).$$

The dc field again brings a slight anisotropy to the harmonic part of potential. Using the result in Eq. (5.5) for a rectangular QD, we obtain the $\varepsilon_x^{(dc)}$ -induced Zeeman energy

$$\delta E_Z^{(dc)}(\tau_v) \approx -\frac{3}{16}\tau_v\mu_{v0}B_{\text{normal}}(k_{4x}x_\varepsilon^{(dc)2})\frac{\hbar w_0}{\Delta}. \quad (6.3)$$

This corresponds to the $\varepsilon_x^{(dc)}$ -induced valley magnetic moment tuning

$$\delta\mu_v^{(dc)} \approx -\mu_{v0}\frac{3}{16}(k_{4x}x_\varepsilon^{(dc)2})\frac{\hbar w_0}{\Delta}. \quad (6.4)$$

In either the cubic or the quadric case, the μ_v tuning can be utilized to create the required asymmetry ($\mu_{vL} \neq \mu_{vR}$) in the DQD structure of the qubit, and generate a qubit state rotation \hat{R}_x about the x axis (of the Bloch sphere). Specifically, we consider the case of a symmetric DQD structure, where $\mu_{vL} = \mu_{vR}$. If a dc electric field is applied on the left QD, for the time t_x , a qubit state $|\Phi\rangle$ will undergo the following rotation [according to Eq. (2.5)]:

$$|\Phi\rangle \rightarrow \hat{R}_x(\theta_x^{(dc)})|\Phi\rangle, \\ \hat{R}_x(\theta_x^{(dc)}) = \exp\left(-i\tau_x\frac{\theta_x^{(dc)}}{2}\right), \quad (6.5) \\ \theta_x^{(dc)} = \Omega_x t_x, \quad \Omega_x = \frac{2}{\hbar}\delta\mu_v^{(dc)}B_{\text{normal}}.$$

Here, we have set the exchange coupling $J \sim 0$ in Eq. (2.5), and replaced $\mu_{vL} - \mu_{vR}$ in the equation with $\delta\mu_v^{(dc)}$ (induced by the field in the left QD). With the parameters $B_{\text{normal}} = 100$ mT, $k_{4x} = L^{-2}$ (L is the QD size), $x_\varepsilon^{(dc)}/L = 0.2$, $-\hbar w_0/\Delta = 0.2$,

$\Delta = 0.14 \text{ eV}$,²⁸ Eqs. (6.4) and (6.5) give Ω_x (the Larmor frequency for \hat{R}_x) $\sim O(\text{ns}^{-1})$, in the typical range currently envisioned in SOI-based spin qubit manipulation.²⁷ This estimate of manipulation speed remains valid when a finite J is included, since, as discussed in Sec. IV, J can reach $O(\text{meV})$, with the corresponding $\Omega_z \gg O(\text{ns}^{-1})$ ($\Omega_z = J/\hbar$, the Larmor frequency for \hat{R}_z).

The ac mode of μ_v tuning can also be achieved with an ac field superimposed on the dc field, e.g.,

$$\varepsilon_x = \varepsilon_x^{(\text{dc})} + \varepsilon_x^{(\text{ac})} \sin(w_{\text{ac}} t).$$

Under the adiabatic condition, e.g., $w_{\text{ac}} \ll w_0$, where the ac field does not cause any transition between QD energy levels, the following additional tuning ($\delta\mu_v^{(\text{ac})}$) is obtained, namely, for weak $\varepsilon_x^{(\text{ac})}$ [$e\varepsilon_x^{(\text{ac})} \ll (\hbar m^* w_0^3)^{1/2}$ in the cubic case, and $\varepsilon_x^{(\text{ac})} \ll \varepsilon_x^{(\text{dc})}$ in the quadric case],

$$\delta\mu_v = \delta\mu_v^{(\text{dc})} + \delta\mu_v^{(\text{ac})}, \quad (6.6)$$

$$\delta\mu_v^{(\text{ac})} \approx -\frac{1}{8}\mu_{v0} (k_{3x} x_\varepsilon^{(\text{ac})}) \sin(w_{\text{ac}} t) \frac{\hbar w_0}{\Delta} \quad (\text{cubic case}), \quad (6.7)$$

$$\delta\mu_v^{(\text{ac})} \approx -\frac{3}{8}\mu_{v0} (k_{4x} x_\varepsilon^{(\text{dc})} x_\varepsilon^{(\text{ac})}) \times \sin(w_{\text{ac}} t) \frac{\hbar w_0}{\Delta} \quad (\text{quadric case}), \quad (6.8)$$

$$x_\varepsilon^{(\text{ac})} \equiv -\frac{e\varepsilon_x^{(\text{ac})}}{m^* w_0^2},$$

correct to the order of $\varepsilon_x^{(\text{ac})}$. This result can be derived by a straightforward application of Eqs. (6.2) and (6.4), where $x_\varepsilon^{(\text{dc})}$ is replaced by $x_\varepsilon^{(\text{dc})} + x_\varepsilon^{(\text{ac})} \sin(w_{\text{ac}} t)$.

We mentioned that the ac mode allows the qubit manipulation via qubit resonance techniques. A simplified picture of the manipulation is given here which involves alternating \hat{R}_x and \hat{R}_z , as follows. We assume that both the QDs are subject to dc fields, and gates V_L and V_R have been tuned such that the dc part of $(\mu_{vL} - \mu_{vR}), (\mu_{vL} - \mu_{vR})^{(\text{dc})}$, vanishes. Moreover, we assume that only the left QD is subject to an ac field, and write the ac part of $(\mu_{vL} - \mu_{vR}), (\mu_{vL} - \mu_{vR})^{(\text{ac})} = \delta\mu_v^{(\text{ac})}$. For one half of the ac cycle, the ac field induces the transformation $|\Phi\rangle \rightarrow_x (\theta_x^{(\text{ac})}) |\Phi\rangle$, with

$$\begin{aligned} \theta_x^{(\text{ac})} &= \frac{2}{\hbar} \int_0^{\pi/w_{\text{ac}}} \delta\mu_v^{(\text{ac})} B_{\text{normal}} dt, \\ \theta_x^{(\text{ac})} &= -\frac{1}{2} k_{3x} x_\varepsilon^{(\text{ac})} \frac{\mu_{v0} B_{\text{normal}} \hbar w_0}{\hbar w_{\text{ac}} \Delta} \quad (\text{cubic case}), \quad (6.9) \\ \theta_x^{(\text{ac})} &= -\frac{3}{2} k_{4x} x_\varepsilon^{(\text{dc})} x_\varepsilon^{(\text{ac})} \frac{\mu_{v0} B_{\text{normal}} \hbar w_0}{\hbar w_{\text{ac}} \Delta} \quad (\text{quadric case}). \end{aligned} \quad (6.10)$$

In the other half of the cycle, it rotates the qubit state through “ $-\theta_x^{(\text{ac})}$ ”. In general, the qubit may be manipulated, e.g., in the alternating sequence $\hat{R}_x(\theta_x^{(\text{ac})}) \rightarrow \hat{R}_z(\theta_z = \pi) \rightarrow \hat{R}_x(-\theta_x^{(\text{ac})}) \rightarrow \hat{R}_z(\theta_z = \pi) \rightarrow \dots \rightarrow \hat{R}_z(\theta_z^{\text{target}} + \pi/2)$, into a target state (θ_z^{target} is the target state longitude). See Fig. 5. Here, we have assumed (1) $J = 0$ when \hat{R}_x is acting on the qubit state, and (2) between the half cycles, the ac field is turned off and J is turned on, for a time length $\pi\hbar/J$, when \hat{R}_z is acting on the qubit state. Under the foregoing assumptions (1) and (2), rotations about the x and z axes are basically decoupled.

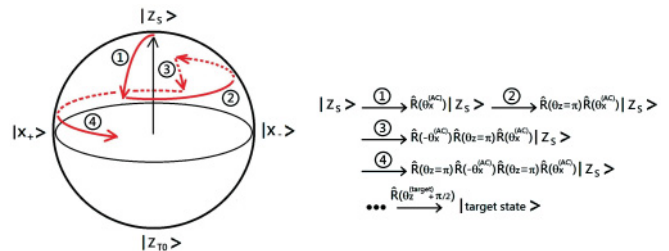


FIG. 5. (Color online) In the ac mode, the initial qubit state, e.g., $|z_s\rangle$, may be manipulated in the alternating sequence $_x(\theta_x^{(\text{ac})}) \rightarrow_z(\theta_z = \pi) \rightarrow_x(-\theta_x^{(\text{ac})}) \rightarrow_z(\theta_z = \pi) \rightarrow \dots \rightarrow_z(\theta_z^{\text{target}} + \pi/2)$ into a target state (θ_z^{target} is the target state longitude).

In the quadric case, the discussion of the ac mode for $\varepsilon_x^{(\text{ac})} \ll \varepsilon_x^{(\text{dc})}$ can be extended to the regime where $\varepsilon_x^{(\text{ac})} \sim \varepsilon_x^{(\text{dc})}$. In order to see this, we write

$$\begin{aligned} \delta\mu_v &= \delta\mu_v^{(\text{dc})} + \delta\mu_v^{(\text{ac})} + \delta\mu_v^{(\text{ac})'}, \\ \delta\mu_v^{(\text{ac})'} &= -\frac{3}{16}\mu_{v0} (k_{4x} x_\varepsilon^{(\text{ac})2}) \sin^2(w_{\text{ac}} t) \frac{\hbar w_0}{\Delta}, \end{aligned}$$

correct to the order of $(\varepsilon_x^{(\text{ac})})^2$. Therefore, an additional term, $\delta\mu_v^{(\text{ac})'}$, arises in the regime. It leads to a rotation through the extra angle

$$\theta_x^{(\text{ac})'} = \frac{2}{\hbar} \int_0^{\pi/w_{\text{ac}}} \delta\mu_v^{(\text{ac})'} B_{\text{normal}} dt$$

in each half of the ac cycle. Being quadratic in $\varepsilon_x^{(\text{ac})}$, the sign of $\theta_x^{(\text{ac})'}$ does not flip during the whole ac cycle. However, this additional rotation is nullified in the alternating sequence of operations, since

$$\hat{R}_x(\theta_x^{(\text{ac})'}) \cdot \hat{R}_z(\theta_z = \pi) \cdot \hat{R}_x(\theta_x^{(\text{ac})'}) = \hat{R}_z(\theta_z = \pi),$$

as can be verified.

Appendix B provides an alternative treatment of the ac electric effect on μ_v by employing a moving reference frame.

VII. THE PHONON-MEDIATED VALLEY RELAXATION IN A QD, AND SINGLET-TRIPLET TRANSITION IN A QD OR DQD

A qubit state may relax or dephase. It constrains the time allowed for qubit manipulation. This issue is discussed below in the case of valley pair qubits.

First, we estimate the valley relaxation time in a QD, in the presence of the normal magnetic field B_{normal} . We take L (the QD size) $\gg \text{\AA}$. The QD-confined states are denoted as $|K_{\text{QD}}\rangle$ and $|K'_{\text{QD}}\rangle$, corresponding to the two energy valleys K and K' , respectively. The valley splitting is written as $\delta E_{KK'}$ ($\sim 2\mu_{v0} B_{\text{normal}}$).

We write $|K_{\text{QD}}\rangle$ and $|K'_{\text{QD}}\rangle$ as follows:

$$|K_{\text{QD}}\rangle = c_{\text{QD}}^{(K)+} |\text{vacuum}\rangle, \quad |K'_{\text{QD}}\rangle = c_{\text{QD}}^{(K')+) |\text{vacuum}\rangle,$$

$$K_{\text{QD}}(\vec{r}) = \langle \vec{r} | K_{\text{QD}} \rangle \approx \phi(\vec{r} - \vec{R}_{\text{QD}}; \tau_v = 1) e^{i\vec{K} \cdot \vec{r}} u_K,$$

$$K'_{\text{QD}}(\vec{r}) = \langle \vec{r} | K'_{\text{QD}} \rangle \approx \phi(\vec{r} - \vec{R}_{\text{QD}}; \tau_v = -1) e^{i\vec{K}' \cdot \vec{r}} u_{K'},$$

$\vec{K} (\vec{K}')$ = wave vector at $K (K')$ point,

$\bar{R}_{\text{QD}} = \text{QD center position,}$

$u_{K(K')} = \text{Bloch cell-periodic function.}$ (7.1)

$c_{\text{QD}}^{(K)+}$ and $c_{\text{QD}}^{(K')\dagger}$ are electron creation operators. Φ is the envelope function, taken to be smoothly varying, with a width L (due to the QD confinement).

The valley relaxation process occurs via the quantum state flip $|K_{\text{QD}}\rangle \leftrightarrow |K'_{\text{QD}}\rangle$. The process involves intervalley scattering between K and K' and hence a corresponding large wave-vector transfer ($\delta k = |\bar{K} - \bar{K}'| \sim \text{\AA}^{-1}$). It may occur easily in the presence of a short-range impurity potential which scatters the electron and provides the required wave-vector difference.³³ In this paper, however, we consider the clean limit where the structure is free of such impurities, and δk must be furnished by the confining QD potential. In addition, because of the energy mismatch $\delta E_{KK'}$ between $|K_{\text{QD}}\rangle$ and $|K'_{\text{QD}}\rangle$, the electron-phonon (EP) interaction also participates in the transition, making up for the energy difference. (This is similar to the phonon-mediated spin relaxation in semiconductor QDs.^{20,21}) Our calculation below is an estimate of the phonon-mediated valley-flip rate in a QD.

The EP interaction is modeled by the deformation potential coupling involving acoustic phonons,

$$H_{\text{EP}} = \sum_Q \sum_{v=K,K'} M_{\text{EP}}^{(v)}(Q)(b_{-Q} + b_Q^\dagger)c_{\text{QD}}^{(v)+}c_{\text{QD}}^{(v)}, \quad (7.2)$$

with the matrix elements

$$M_{\text{EP}}^{(K)}(Q) = D|Q|\sqrt{\frac{\hbar}{2\rho_a A w_Q}} \langle K_{\text{QD}} | e^{i\vec{Q}\cdot\vec{r}} | K_{\text{QD}} \rangle, \quad (7.3)$$

$$M_{\text{EP}}^{(K')}(Q) = D|Q|\sqrt{\frac{\hbar}{2\rho_a A w_Q}} \langle K'_{\text{QD}} | e^{i\vec{Q}\cdot\vec{r}} | K'_{\text{QD}} \rangle.$$

b and b^\dagger are phonon creation and annihilation operators, D is the deformation potential constant, Q is the phonon wave vector, ρ_a is the mass density, A is the system area, $w_Q = c_s Q$ (acoustic phonon dispersion), and c_s is the sound velocity.

The QD potential is written below:

$$V_{\text{QD}} \approx M_{\text{QD}}^{(KK')} c_{\text{QD}}^{(K)+} c_{\text{QD}}^{(K')\dagger} + \text{H.c.},$$

$$M_{\text{QD}}^{(KK')} = \langle K_{\text{QD}} | V_{\text{QD}} | K'_{\text{QD}} \rangle, \quad M_{\text{QD}}^{(K'K)} = \langle K'_{\text{QD}} | V_{\text{QD}} | K_{\text{QD}} \rangle. \quad (7.4)$$

We take the depth of V_{QD} to be V_0 . We estimate

$$|M_{\text{QD}}^{(KK')}| \approx |M_{\text{QD}}^{(K'K)}| \approx M_{\text{QD}}, \quad M_{\text{QD}} = \frac{V_0}{1 + (L\delta k)^2}. \quad (7.5)$$

The Lorentzian function with a width $1/L$ is used here and below for the Fourier transform of a \vec{r} -space function with spatial width $\sim L$.

The phonon-mediated valley flip $|K_{\text{QD}}\rangle \leftrightarrow |K'_{\text{QD}}\rangle$ is a second-order process involving the following products of matrix elements:

$$\begin{aligned} & \langle K'_{\text{QD}} | Q | H_{\text{EP}} | K'_{\text{QD}} \rangle \langle K'_{\text{QD}} | V_{\text{QD}} | K_{\text{QD}} \rangle, \\ & \langle K'_{\text{QD}} | Q | V_{\text{QD}} | K_{\text{QD}} \rangle \langle K_{\text{QD}} | Q | H_{\text{EP}} | K_{\text{QD}} \rangle \end{aligned} \quad (7.6)$$

(both with phonon emission),

or

$$\begin{aligned} & \langle K_{\text{QD}} | H_{\text{EP}} | K_{\text{QD}} \rangle \langle K_{\text{QD}} | Q | V_{\text{QD}} | K'_{\text{QD}} \rangle, \\ & \langle K_{\text{QD}} | V_{\text{QD}} | K'_{\text{QD}} \rangle \langle K'_{\text{QD}} | H_{\text{EP}} | K'_{\text{QD}} \rangle \end{aligned} \quad (7.7)$$

(both with phonon absorption).

Composite electron-phonon states appear here. For instance, $|K_{\text{QD}}, Q\rangle$ denotes the one-electron (K_{QD})–one phonon (Q) state.

For the transition $|K_{\text{QD}}\rangle \leftrightarrow |K'_{\text{QD}}\rangle$, Fermi's golden rule gives the rate

$$\begin{aligned} \frac{1}{\tau_{K' \rightarrow K}} &= \frac{2\pi}{\hbar} \sum_Q n_Q |M_{K' \rightarrow K}|^2 \delta(|\delta E_{KK'}| - \hbar w_Q) \\ & \quad (\text{with phonon absorption}), \\ \frac{1}{\tau_{K \rightarrow K'}} &= \frac{2\pi}{\hbar} \sum_Q (n_Q + 1) |M_{K \rightarrow K'}|^2 \delta(|\delta E_{KK'}| - \hbar w_Q) \\ & \quad (\text{with phonon emission}). \end{aligned} \quad (7.8)$$

Here, n_Q is the average phonon occupation number, and $M_{K' \rightarrow K}$ and $M_{K \rightarrow K'}$ are the effective matrix elements describing the second-order processes in Eqs. (7.6) and (7.7), respectively, with

$$\begin{aligned} & |M_{K' \rightarrow K}| \\ & \approx |M_{K \rightarrow K'}| \approx \frac{1}{|\delta E_{KK'}|} |M_{\text{QD}}| |M_{\text{EP}}^{(K)}(Q) - M_{\text{EP}}^{(K')}(Q)|. \end{aligned} \quad (7.9)$$

For $B_{\text{normal}} = 0$, the EP part in Eq. (7.9) vanishes due to the time-reversal symmetry. For a finite B_{normal} , the EP part is finite, and an upper bound estimate is given below. (A more accurate estimate is given later.) We write

$$\begin{aligned} & |M_{\text{EP}}^{(K)}(Q) - M_{\text{EP}}^{(K')}(Q)| \\ & \leq O(|M_{\text{EP}}^{(K)}(Q)|) \quad [\text{or } O(|M_{\text{EP}}^{(K')}(Q)|)], \\ & |M_{\text{EP}}^{(K)}(Q)| \approx |M_{\text{EP}}^{(K')}(Q)| \approx \frac{D}{1 + L^2 Q^2} \sqrt{\frac{\hbar|Q|}{2\rho_a A c_s}} \quad [\equiv M_{\text{EP}}(Q)]. \end{aligned} \quad (7.10)$$

Using Eq. (7.10), we obtain

$$\begin{aligned} \frac{1}{\tau_{K \leftrightarrow K'}} &\leq O(1) \frac{2\pi}{\hbar} \left(\frac{1}{\delta E_{KK'}} \right)^2 \sum_Q \left(n_Q + \frac{1}{2} \pm \frac{1}{2} \right) \\ & \quad \times M_{\text{QD}}^2 M_{\text{EP}}^2 \delta(|\delta E_{KK'}| - \hbar w_Q). \end{aligned} \quad (7.11)$$

After performing the Q summation, we obtain

$$\begin{aligned} \frac{1}{\tau_{K \leftrightarrow K'}} &\leq O(1) \frac{V_0^2 D^2}{\hbar^3 c_s^4 \rho_a (1 + L^2 \delta k^2)^2 (1 + L^2 Q_0^2)^2} \\ & \quad \times \left(n_{Q_0} + \frac{1}{2} \pm \frac{1}{2} \right), \end{aligned} \quad (7.12)$$

$$\hbar c_s Q_0 = |\delta E_{KK'}|.$$

Now, we give a more accurate estimate of the relaxation rate for weak B_{normal} . We expect the EP part $[M_{\text{EP}}^{(K)}(Q) - M_{\text{EP}}^{(K')}(Q)]$ in Eq. (7.9) to be linear in B_{normal} at weak B_{normal} . Therefore, for the estimate, we need to calculate each of the

EP matrix elements correct to the order of B_{normal} . According to Eq. (7.3), this requires the calculation of the states $|K_{\text{QD}}\rangle$ and $|K'_{\text{QD}}\rangle$ correct to the same order.

We use the Hamiltonian given earlier and listed again here,

$$\begin{aligned} H &\simeq H_{B\tau}^{(0)} + H_{B0}^{(0)} + H_{0\tau}^{(1)} + H_{B\tau}^{(1)} + H_{\text{rest}}, \\ H_{B\tau}^{(0)} &= \frac{\vec{p}^2}{2m^*} + V + \tau_v \mu_{v0} B_{\text{normal}}, \quad H_{B0}^{(0)} = \frac{e\vec{A} \cdot \vec{p}}{m^*}, \\ H_{0\tau}^{(1)} &= \tau_v \frac{\hbar}{4m^* \Delta} [(\nabla V) \times \vec{p}]_{\text{normal}}, \\ H_{B\tau}^{(1)} &= -\tau_v \mu_{v0} \left(B_{\text{normal}} \frac{\vec{p}^2}{2m^* \Delta} + \frac{1}{2\Delta} [\vec{A} \times (\nabla V)]_{\text{normal}} \right). \end{aligned}$$

We take $V = V_{\text{QD}}(r) = \frac{1}{2} m^* w_0^2 r^2$. A perturbative calculation using the symmetric gauge $(A_x, A_y) = \frac{1}{2}(-B_{\text{normal}}y, B_{\text{normal}}x)$ yields the following ground-state wave function $[\Phi_{00}(\tau_v = 1)]$ for the state $|K_{\text{QD}}\rangle$ and $\Phi_{00}(\tau_v = -1)$ for $|K'_{\text{QD}}\rangle$ correct to $O(B_{\text{normal}})$,

$$\begin{aligned} \phi_{00}(\tau_v) &= \phi_{00}^{(0)} + \delta\phi_{B\tau} + \delta\phi_{\text{rest}}, \\ \delta\phi_{B\tau} &= \sum_{nm \neq 00} \frac{\langle \phi_{nm}^{(0)} | H_{B\tau}^{(1)} | \phi_{00}^{(0)} \rangle}{E_{00}^{(0)}(\tau_v) - E_{nm}^{(0)}(\tau_v)} \phi_{nm}^{(0)} \\ &= -\frac{3\sqrt{2}}{16} \tau_v \frac{\mu_{v0} B_{\text{normal}}}{\Delta} (\phi_{20}^{(0)} + \phi_{02}^{(0)}), \\ H_{B\tau}^{(0)} \phi_{nm}^{(0)} &= E_{nm}^{(0)} \phi_{nm}^{(0)}. \end{aligned} \quad (7.13)$$

$\Phi_{nm}^{(0)}$ is the 2D isotropic oscillator wave function. $\delta\Phi_{\text{rest}}$ is the part of perturbative correction that does not depend on either τ_v or B_{normal} . Since $[M_{\text{EP}}^{(K)}(Q) - M_{\text{EP}}^{(K')}(Q)]$ is expected to be linear in B_{normal} , $\delta\Phi_{\text{rest}}$ is irrelevant for the calculation. Using $\Phi_{00}(\tau_v)$ in Eq. (7.13), we calculate $[M_{\text{EP}}^{(K)}(Q) - M_{\text{EP}}^{(K')}(Q)]$ according to Eq. (7.3),

$$\begin{aligned} M_{\text{EP}}^{(K)}(Q) - M_{\text{EP}}^{(K')}(Q) &\approx \frac{3}{8} D \frac{\hbar}{m^* w_0} \frac{\mu_{v0} B_{\text{normal}}}{\Delta} |Q|^3 e^{-(\hbar Q^2/4m^* w_0)} \sqrt{\frac{\hbar}{2\rho_a A w_Q}}. \end{aligned} \quad (7.14)$$

When we substitute this result into Eq. (7.9), and (7.9) into (7.8), it gives

$$\begin{aligned} \frac{1}{\tau_{K \leftrightarrow K'}} &\approx O(1) \left(n_{Q_0} + \frac{1}{2} \pm \frac{1}{2} \right) \frac{\mu_{v0}^2}{e^2 \hbar^5 \rho_a c_s^8} \\ &\times \frac{1}{(1 + \delta k^2 L^2)^2} \frac{V_0^2 D^2}{(\hbar w_0 \Delta)^2} e^{-(\hbar Q_0^2/2m^* w_0)} (\mu_{v0} B_{\text{normal}})^6 \\ &(+ \text{ for phonon emission, } - \text{ for phonon absorption}), \\ \hbar c_s Q_0 &= |\delta E_{KK'}| \left(\text{for } B_{\text{normal}} < \frac{\hbar w_0}{2\mu_{v0}} \right). \end{aligned} \quad (7.15)$$

The condition $B_{\text{normal}} < w_0/2\mu_{v0}$ is imposed here to avoid level crossing between the lowest K orbital and the first excited K' orbital. For $\Delta = 0.14$ eV, $L \sim 350$ Å, $w_0 \sim 30$ meV, this condition is satisfied for $B_{\text{normal}} < 6.7$ T. Using these parameters, together with $V_0 \sim 0.5\Delta$ (for a bound state to exist), $D = 18$ eV,³⁴ $c_s = 2.1 \times 10^4$ m/s,³⁴

$B_{\text{normal}} = 100$ mT, and a temperature of 10 K, we obtain $\tau_{K \leftrightarrow K'} \sim O$ (ms), sufficiently long for qubit manipulation. The time scale here for the valley relaxation is the same as that for the SOI-induced spin decay in InAs nanowire QDs.³⁵ If Eq. (7.15) is extrapolated to the regime of room temperatures, it gives $T_1 \sim O(10 \mu\text{s})$.

The discussion of valley relaxation can be generalized to the singlet-triplet transition $|z_S\rangle \leftrightarrow |z_{T\pm}\rangle$ in the DQD structure. It yields

$$\begin{aligned} \frac{1}{\tau_{S \leftrightarrow T\pm}} &= \frac{2\pi}{\hbar} \sum_Q \left(n_Q + \frac{1}{2} \mp \frac{1}{2} \right) \\ &\times |M_{S \rightarrow T\pm}|^2 \delta(|\delta E_{ST\pm}| - \hbar w_Q). \end{aligned} \quad (7.16)$$

Here, $\delta E_{ST\pm} = E_S - E_{T\pm}$ (singlet-triplet energy difference). The singlet and triplet states are listed earlier in Sec. II.

The transition $|z_S\rangle \leftrightarrow |z_{T\pm}\rangle$ is also a second-order process [similar to those given in Eqs. (7.6) and (7.7)] and involves the phonon-mediated valley flip. $M_{S \rightarrow T+}$ and $M_{S \rightarrow T-}$ in Eq. (7.16) are the corresponding effective matrix elements of the process, with

$$\begin{aligned} M_{S \rightarrow T+} &= \frac{1}{2\sqrt{2}} \frac{1}{\delta E_{ST+}} (M_{\text{QD},R}^{(KK')} - M_{\text{QD},L}^{(KK')}) [M_{\text{EP},L}^{(K)}(Q) \\ &+ M_{\text{EP},R}^{(K)}(Q) - M_{\text{EP},L}^{(K')}(Q) - M_{\text{EP},R}^{(K')}(Q)] \end{aligned} \quad (7.17)$$

and

$$\begin{aligned} M_{S \rightarrow T-} &= \frac{1}{2\sqrt{2}} \frac{1}{\delta E_{ST-}} (M_{\text{QD},L}^{(K'K)} - M_{\text{QD},R}^{(K'K)}) [M_{\text{EP},L}^{(K)}(Q) \\ &+ M_{\text{EP},R}^{(K)}(Q) - M_{\text{EP},L}^{(K')}(Q) - M_{\text{EP},R}^{(K')}(Q)]. \end{aligned}$$

The matrix elements appearing here are defined by expressions similar to those in Eqs. (7.3) and (7.13), modified to take into account that there are now left and right QDs involved, e.g.,

$$\begin{aligned} M_{\text{EP},\chi}^{(K)}(Q) &= D|Q| \sqrt{\frac{\hbar}{2\rho_a A w_Q}} \langle K_\chi | e^{i\vec{Q} \cdot \vec{r}} | K_\chi \rangle, \\ M_{\text{EP},\chi}^{(K')}(Q) &= D|Q| \sqrt{\frac{\hbar}{2\rho_a A w_Q}} \langle K'_\chi | e^{i\vec{Q} \cdot \vec{r}} | K'_\chi \rangle, \\ M_{\text{QD},\chi}^{(KK')} &= \langle K_\chi | V_{\text{QD}}^{(\chi)} | K'_\chi \rangle, \quad M_{\text{QD},\chi}^{(K'K)} = \langle K'_\chi | V_{\text{QD}}^{(\chi)} | K_\chi \rangle, \\ &\chi = L \text{ (left) or } R \text{ (right) (QD)}. \end{aligned} \quad (7.18)$$

$V_{\text{QD}}^{(L)}$ and $V_{\text{QD}}^{(R)}$ are the confinement potentials of the left and right QDs, respectively.

If the left and right QDs are identical, the QD potential part in $M_{S \rightarrow T\pm}$ vanishes. In general, for dissimilar left and right QDs (with comparable size $\sim L$), we may write

$$\begin{aligned} |M_{S \rightarrow T\pm}| &< O(1) \frac{1}{|\delta E_{ST\pm}|} \\ &\times M_{\text{QD}} |M_{\text{EP}}^{(K)}(Q) - M_{\text{EP}}^{(K')}(Q)|. \end{aligned} \quad (7.19)$$

This is analogous to the matrix element in Eq. (7.9) for valley flip, and, when used in Eq. (7.16), leads to Eq. (7.15) (with the substitution $\delta E_{KK'} \rightarrow \delta E_{ST\pm}$) as an upper bound estimate of $1/\tau_{S \leftrightarrow T\pm}$, giving $\tau_{S \leftrightarrow T\pm} > O$ (ms).

A similar calculation applies to the transition $|z_S\rangle \leftrightarrow |z_{T\pm}\rangle$ in a single QD. This case is relevant if the valley qubit is initialized by utilizing one-QD singlets, as in the case of spin-pair scheme.¹³ The transition rate is again described by Eq. (7.16), and the matrix element involved is discussed in the following.

The singlet and triplet states are written below:

$$\begin{aligned} |z_S\rangle &= c_{\text{QD}}^{(K_0)+} c_{\text{QD}}^{(K'_0)+} |\text{vacuum}\rangle, \\ |z_{T+}\rangle &= c_{\text{QD}}^{(K_0)+} c_{\text{QD}}^{(K_1)+} |\text{vacuum}\rangle, \\ |z_{T-}\rangle &= c_{\text{QD}}^{(K'_1)+} c_{\text{QD}}^{(K'_0)+} |\text{vacuum}\rangle. \end{aligned} \quad (7.20)$$

Here, the index 0 represents the lowest orbital, and 1 represents the first excited one. The effective matrix element for the transition is

$$\begin{aligned} M_{S \rightarrow T+} &= \frac{1}{\delta E_{ST+}} M_{\text{QD}}^{(K_1 K'_0)} [M_{\text{EP}}^{(K_1)}(Q) - M_{\text{EP}}^{(K'_0)}(Q)], \\ M_{S \rightarrow T-} &= \frac{1}{\delta E_{ST-}} M_{\text{QD}}^{(K'_1 K_0)} [M_{\text{EP}}^{(K'_1)}(Q) - M_{\text{EP}}^{(K_0)}(Q)], \\ M_{\text{QD}}^{(K_1 K'_0)} &= \langle K_1 | V_{\text{QD}} | K'_0 \rangle, \quad M_{\text{QD}}^{(K'_1 K_0)} = \langle K'_1 | V_{\text{QD}} | K_0 \rangle, \\ M_{\text{EP}}^{(K_i)}(Q) &= DQ \sqrt{\frac{\hbar}{2\rho_a A w_Q}} \langle K_i | e^{i\vec{Q}\cdot\vec{r}} | K_i \rangle, \\ M_{\text{EP}}^{(K'_i)}(Q) &= DQ \sqrt{\frac{\hbar}{2\rho_a A w_Q}} \langle K'_i | e^{i\vec{Q}\cdot\vec{r}} | K'_i \rangle, \quad i = 0, 1. \end{aligned} \quad (7.21)$$

For a symmetric QD in the absence of magnetic field, the lowest and the first excited orbitals have opposite parity symmetry. It follows that $M_{\text{QD}}^{(K_1 K'_0)} = M_{\text{QD}}^{(K'_1 K_0)} = 0$ and, thereby, $M_{S \rightarrow T+}$ and $M_{S \rightarrow T-}$ both vanish. In the general case where the QD is asymmetric, we employ the following approximation:

$$|M_{S \rightarrow T\pm}| \rightarrow O(1) \frac{1}{|\delta E_{ST\pm}|} M_{\text{QD}} M_{\text{EP}}. \quad (7.22)$$

This leads to Eqs. (7.11) and (7.12) (with the substitution $\delta E_{KK'} \rightarrow \delta E_{ST\pm}$) as an estimate for $1/\tau_{ST\pm}$. Using $\Delta \sim 0.14$ eV, $L \sim 350$ Å, $V_0 \sim 0.5\Delta$ (for a bound state to exist), $\delta E_{ST\pm} \sim 30$ meV, $B_{\text{normal}} \sim 100$ mT, and a temperature of 10 K, we obtain $\tau_{S \leftrightarrow T\pm} \gg O(\text{ms})$.

Last, we discuss shortly the singlet-triplet transition $|z_S\rangle \leftrightarrow |z_{T0}\rangle$ in the DQD. The transition is caused only by the EP interaction, and does not involve any valley flip. The energy difference between the states is J (the exchange splitting). The transition rate is given below:

$$\begin{aligned} \frac{1}{\tau_{S \leftrightarrow T_0}} &= \frac{2\pi}{\hbar} \sum_Q \left(n_Q + \frac{1}{2} \pm \frac{1}{2} \right) |M_{S \rightarrow T_0}|^2 \delta(J - \hbar w_Q) \\ & \quad (+ \text{ for } T_0 \rightarrow S, \quad - \text{ for } S \rightarrow T_0), \end{aligned} \quad (7.23)$$

with the matrix element

$$\begin{aligned} M_{S \rightarrow T_0} &= \frac{1}{2} [M_{\text{EP},L}^{(K)}(Q) - M_{\text{EP},R}^{(K)}(Q) - M_{\text{EP},L}^{(K')}(Q) \\ & \quad + M_{\text{EP},R}^{(K')}(Q)]. \end{aligned} \quad (7.24)$$

For identical left and right QDs, the matrix element vanishes. In the general case where the QDs are dissimilar (with comparable size $\sim L$), we may follow the calculation that leads to Eq. (7.14), and write

$$M_{S \rightarrow T_0} \approx O(1) D \frac{(\mu_{vL} - \mu_{vR}) B_{\text{normal}}}{m^* w_0^2} |Q|^3 e^{-(\hbar Q^2 / 4m^* w_0)} \sqrt{\frac{\hbar}{2\rho_a A w_Q}}. \quad (7.25)$$

This gives

$$\begin{aligned} \frac{1}{\tau_{S \leftrightarrow T_0}} &\approx O(1) \left(n_{Q_0} + \frac{1}{2} \pm \frac{1}{2} \right) \frac{\mu_{v0}^2}{e^2 \hbar^5 \rho_a c_s^8} \frac{D^2 J^6}{(\hbar w_0)^4} \\ &\quad \times e^{-(\hbar Q_0^2 / 2m^* w_0)} [(\mu_{vL} - \mu_{vR}) B_{\text{normal}}]^2, \quad \hbar c_s Q_0 = J. \end{aligned} \quad (7.26)$$

We use Eq. (7.26) to estimate $\tau_{S \leftrightarrow T_0}$. We take $(\mu_{vL} - \mu_{vR}) B_{\text{normal}} \sim 1$ μeV, $L \sim 350$ Å, $D \sim 18$ eV, $\hbar w_0 \sim 30$ meV, and a temperature ~ 10 K. For the stage of ac mode manipulation when the rotation \hat{R}_z is acting on the qubit state, we take $J \sim 0.1$ meV. On the other hand, for the stage when the rotation \hat{R}_x is acting on the qubit state, we take $J \sim 0.1$ μeV. In either case, it gives $\tau_{S \leftrightarrow T_0} \gg O(\text{ms})$.

In conclusion, the discussion in this section shows that the qubit coherence time is $O(\text{ms})$ in a typical case.

VIII. SUMMARY

In summary, this paper has examined the physics underlying valley pair qubits in graphene DQDs. Confined valley magnetic moments can be modulated electrically in dc or ac modes based on the analog of first-order relativistic effect in graphene, with the distinctive advantage of being state-mixing free. This mechanism, together with the electrically tunable exchange coupling, allows all-electric manipulation of qubits via electric gates, on the time scale of ns. Moreover, the qubits envisioned here are fault tolerant, with a long coherence time $\sim O(\text{ms})$.

Implementation of valley pair qubits requires the capabilities to (1) open a gap in graphene, and (2) manufacture gated graphene devices in the nanometer scale, both being important issues in the current development of graphene-based nanoelectronics. Experimental realization of the qubits will lead to utilization of the valley DOF, in addition to the spin DOF, in quantum information encoding, and raise the interesting prospect of valley-based quantum computing and communication in carbon systems.

ACKNOWLEDGMENTS

We thank the support of ROC National Science Council through Contract No. NSC-99-2112-M-007-019.

APPENDIX A: DERIVATION OF THE SCHRÖDINGER-TYPE EQUATION FOR ELECTRONS IN GAPPED GRAPHENE

We sketch the derivation of the Schrödinger-type equation in gapped graphene, with the magnetic effect and the first-order R.C. included.

We begin with the Dirac-type equation

$$H_D \phi_D = E \phi_D,$$

$$H_D = \begin{pmatrix} \Delta + V & v_F \hat{\pi}_- \\ v_F \hat{\pi}_+ & -\Delta + V \end{pmatrix}, \quad \phi_D = \begin{pmatrix} \phi_A \\ \phi_B \end{pmatrix}, \quad (\text{A1})$$

$$\begin{aligned} \vec{\pi} &= \vec{p} + e\vec{A}, \quad \vec{A} = \frac{1}{2}(-B_{\text{normal},y}, B_{\text{normal},x}), \\ \hat{p}_+ &= \hat{p}_x + i\tau_v \hat{p}_y, \quad \hat{p}_- = \hat{p}_x - i\tau_v \hat{p}_y, \\ A_+ &= A_x + i\tau_v A_y, \quad A_- = A_x - i\tau_v A_y, \\ \hat{\pi}_+ &= \hat{p}_+ + eA_+, \quad \hat{\pi}_- = \hat{p}_- + eA_-. \end{aligned}$$

Solving (A1), we obtain the following relation between the two components of Φ_D ,

$$\phi_B = \frac{1}{\Delta + E - V} v_F \hat{\pi}_+ \phi_A, \quad (\text{A2})$$

and the following equation for the component Φ_A ,

$$\begin{aligned} H_N \phi_A &= (E - \Delta) \phi_A, \\ H_N &= v_F \hat{\pi}_- \left(\frac{1}{\Delta + E - V} v_F \hat{\pi}_+ \right) + V. \end{aligned} \quad (\text{A3})$$

Equation (A3) contains full relativistic effects. It can be reduced to the Schrödinger equation with only the first-order R.C. included, as follows.

We expand $\frac{1}{\Delta + E - V}$ in Eq. (A3), and keep the R.C. up to the first order,

$$\begin{aligned} H_N \phi_A &\approx v_F \hat{\pi}_- \frac{1}{2\Delta} \left[1 - \frac{E - \Delta - V}{2\Delta} \right] v_F \hat{\pi}_+ \phi_A + V \phi_A, \\ &= (H_N^{(0)} + H_N^{(1)}) \phi_A. \\ H_N^{(0)} \phi_A &= v_F \hat{\pi}_- \frac{1}{2\Delta} v_F \hat{\pi}_+ \phi_A + V \phi_A, \quad (\text{A4}) \\ H_N^{(1)} \phi_A &= -v_F \hat{\pi}_- \frac{1}{2\Delta} \left(\frac{E - \Delta - V}{2\Delta} \right) v_F \hat{\pi}_+ \phi_A \\ &\quad (\text{first-order R.C.}). \end{aligned} \quad (\text{A5})$$

$H_N^{(0)}$ is the nonrelativistic part of the Hamiltonian, and $H_N^{(1)}$ is the first-order R.C. $H_N^{(0)}$ in Eq. (A4) is further simplified with the following identity:

$$\hat{\pi}_- (\hat{\pi}_+ f) = \hat{\pi}^2 f + 2m^* \tau_v \mu_{v0} B_{\text{normal}} f \quad (f = \text{generic expression}). \quad (\text{A6})$$

This gives

$$H_N^{(0)} = \frac{\vec{\pi}^2}{2m^*} + V + \tau_v \mu_{v0} B_{\text{normal}}. \quad (\text{A7})$$

$H_N^{(1)}$ in Eq. (A5) is also simplified, with the following identity:

$$(E - \Delta - V) \hat{\pi}_+ \phi_A = \hat{\pi}_+ ((E - \Delta - V) \phi_A) + (\hat{p}_+ V) \phi_A,$$

where the first term on the right-hand side is further replaced, e.g., $(E - \Delta - V) \phi_A \rightarrow v_F \hat{\pi}_- \left(\frac{1}{\Delta + E - V} v_F \hat{\pi}_+ \phi_A \right) \approx \frac{1}{2m^*} \hat{\pi}_- \hat{\pi}_+ \phi_A$, according to Eq. (A3). This yields

$$\begin{aligned} H_N^{(1)} &= -\frac{1}{2\Delta} \left(\frac{\vec{\pi}^2}{2m^*} + \tau_v \mu_{v0} B_{\text{normal}} \right)^2 \\ &\quad + \frac{\hbar \tau_v}{4m^* \Delta} [(\nabla V) \times \vec{\pi}]_{\text{normal}} \\ &\quad - \frac{e}{4m^* \Delta} \vec{A} \cdot (\vec{p} V) - \frac{1}{4m^* \Delta} (\vec{p} V) \cdot \vec{p} - \frac{1}{4m^* \Delta} (\vec{p}^2 V), \end{aligned} \quad (\text{A8})$$

Note that $H_N^{(1)}$ includes non-Hermitian terms, such as $\frac{1}{4m^* \Delta} \left(\frac{-V}{p} \right) \cdot \vec{p}$. A similar situation also arises in the derivation of a Schrödinger equation (with the first-order R.C. included) from the Dirac equation, in relativistic quantum mechanics, with the reason being that Φ_A is not really the corresponding Schrödinger wave function. It is a component of the Dirac wave function Φ_D and, moreover, not even normalized to the first-order R.C. We follow the standard procedure in the textbook (see, for example, Ref. 36) to deal with the situation. We apply the following similarity transformation:

$$\begin{aligned} \phi_A \rightarrow \phi &= \Omega \phi_A, \quad H_N \rightarrow H = \Omega H_N \Omega^{-1}, \\ \Omega &= 1 + \frac{1}{8m^* \Delta} \hat{\pi}^2. \end{aligned} \quad (\text{A9})$$

It can be verified that the function Φ is normalized to the first-order R.C. The transformation in Eq. (A9) converts H_N into the following Hermitian Hamiltonian H with

$$\begin{aligned} H \phi &= E \phi, \\ H &= H^{(0)} + H^{(1)}, \\ H^{(0)} &= \frac{\vec{\pi}^2}{2m^*} + V + \tau_v \mu_{v0} B_{\text{normal}}, \\ H^{(1)} &= R_1^{(1)} + R_2^{(1)}, \quad (\text{A10}) \\ R_1^{(1)} &= \frac{\hbar \tau_v}{4m^* \Delta} [(\nabla V) \times \vec{\pi}]_{\text{normal}} \quad (\text{VOI}), \\ R_2^{(1)} &= -\frac{1}{2\Delta} \left(\frac{\vec{\pi}^2}{2m^*} + \tau_v \mu_{v0} B_{\text{normal}} \right)^2 - \frac{1}{8m^* \Delta} (\vec{p}^2 V). \end{aligned}$$

(The electron energy E here is defined with respect to the conduction-band edge.)

It is noted that our derivation here is a close analog of the Foldy-Wourhuyawn representation of the Dirac equation. Since the valley degree of freedom here plays a similar role to the electron spin, it is not a surprise that the VOI—the analog of SOI—appears in the Schrödinger-type equation derived above.

APPENDIX B: AN ALTERNATIVE TREATMENT OF THE AC ELECTRIC EFFECT ON μ_v

An alternative treatment of the ac electric effect on μ_v is provided here employing a moving reference frame. We consider a QD in the presence of both a normal magnetic field (B_{normal}) and an in-plane ac electric field [$\varepsilon_x^{(\text{ac})} \sin(\omega_{\text{ac}} t)$ in the x direction].

First, we investigate the case where the confining potential is dominantly quadratic but asymmetric with an anharmonic x^3 term,

$$\begin{aligned} H \phi &\approx (H^{(0)} + H^{(1)}) \phi, \\ V &= V_{\text{QD}}(x, y, t) + e \varepsilon_x^{(\text{ac})} x \sin(\omega_{\text{ac}} t), \\ V_{\text{QD}}(x, y, t) &= V_2(x, y, t) + V_3(x, y, t), \\ V_2(x, y, t) &= \frac{m^* \omega_0^2}{2} (x^2 + y^2), \quad V_3(x, y, t) = \frac{m^* \omega_0^2}{3} k_{3x} x^3. \end{aligned}$$

Here $H^{(0)}$ and $H^{(1)}$ are those given earlier, e.g., in Appendix A. k_{3x} characterizes the strength of V_3 . We assume weak k_{3x} [$k_{3x} \ll (m^*w_0/\hbar)^{1/2}$] in order to facilitate the perturbative argument below. We also assume the adiabatic condition, namely,

$$w_{ac} \ll w_0,$$

meaning that the electron displacement occurs on a time scale much slower than that of the orbital motion.

The potential minimum location $[x_0(t), 0]$ [$x_0(t) = x_\varepsilon^{(ac)} \sin(w_{ac}t)$, $x_\varepsilon^{(ac)} = -\frac{e\varepsilon_x^{(ac)}}{m^*w_0^2}$] varies in time, due to the ac field. Let $\varepsilon_x^{(ac)}$ be weak [$e\varepsilon_x^{(ac)} \ll (\hbar m^*w_0^3)^{1/2}$]. We write

$$V \approx V_2 [x - x_0(t), y, t] + V_3 [x - x_0(t), y, t] + V_{2x} [x - x_0(t), y, t], \quad (\text{B1})$$

$$V_{2x}(x, y, t) = k_{3x}x_0(t)m^*w_0^2x^2,$$

correct to the order of x_0 . V_{2x} modifies the quadratic part of confining potential in the x direction, giving the frequency parameter

$$w_0 \rightarrow w_x = w_0 \left(1 + \frac{\delta w_x}{w_0}\right), \quad \delta w_x = k_{3x}x_0(t)w_0. \quad (\text{B2})$$

Because of the adiabatic condition $w_{ac} \ll w_0$, the problem here can be regarded as quasi-time independent, on the time scale of the orbital motion. We are particularly interested in the energy shift caused by the ac field. For the study of μ_v tuning, we focus on the part of the shift, denoted as δE_{LiVCS} , which is linear in both $\varepsilon_x^{(ac)}$ and B_{normal} , as well as valley dependent, i.e.,

$$\delta E_{\text{LiVCS}} \propto \tau_v \varepsilon_x^{(ac)} B_{\text{normal}}.$$

(LiVCS means ‘‘linear valley-contrasting energy shift’’.)

We reformulate the present problem in a moving reference frame, with the following transformation:

$$x \rightarrow x' = x - x_0(t), \quad f(x, y; t) \rightarrow f'(x', y; t)$$

(f is a generic expression). It leads to the equation (in the moving frame)

$$\begin{aligned} H' \psi'(x', y'; t) &= i\hbar \partial_t \psi'(x', y'; t), \\ H' &= H^{(0')} + V_{2x}' + H^{(1)'} - v_{x0} \hat{p}_{x'}, \\ v_{x0} &\equiv \partial_t x_0 \propto \varepsilon_x^{(ac)}. \end{aligned}$$

With the adiabatic condition, we regard H' as being quasi-time independent, and discuss the effects of $\varepsilon_x^{(ac)}$ -dependent terms, i.e., V_{2x}' and $v_{x0} \hat{p}_{x'}$, within the time-independent perturbation theory. We write the corresponding time-independent wave equation

$$\begin{aligned} H' \phi'(x', y') &= E \phi'(x', y'), \\ H' &= H^{(0')} + V_{2x}' + H^{(1)'} - v_{x0} \hat{p}_{x'}. \end{aligned}$$

First, we estimate the effect of the term $v_{x0} \hat{p}_{x'}$. We note that

$$E(\tau_v, x_0, v_{x0}) = E(\tau_v, x_0, -v_{x0}).$$

[We regard x_0 and v_{x0} as independent parameters in H' . Given $V'(x', y) = V'(x', -y)$ here, it can be verified that if

$\Phi'(x', y)$ is an eigenstate of $H'(\tau_v, x_0, v_{x0})$ with energy E , then $\Phi^*(x', -y)$ is an eigenstate of $H'(\tau_v, x_0, -v_{x0})$ with the same energy E .] It shows that the effect of the term on the energy is of the order of v_{x0}^2 ($\propto \varepsilon_x^{(ac)2}$) or of a higher order, and does not contribute to δE_{LiVCS} . We thereby drop this term below. (From here on, we also drop the prime notation whenever it does not cause confusion.)

Thereby, we write

$$H \approx H^{(0)} + H^{(1)} + V_{2x}. \quad (\text{B3})$$

The presence of V_{2x} shows that the quadratic part of V_{QD} is modified, as described in Eqs. (B1) and (B2), into one with a slight anisotropy describing a rectangular QD. Now, Eq. (5.5) for a rectangular QD can be applied. We obtain

$$\begin{aligned} \delta E_{\text{LiVCS}} &= \tau_v \delta \mu_v^{(ac)} B_{\text{normal}}, \\ \delta \mu_v^{(ac)} &= -\frac{1}{8} \mu_{v0} (k_{3x} x_\varepsilon^{(ac)}) \sin(w_{ac}t) \left(\frac{\hbar w_0}{\Delta} \right) \quad (\text{cubic case}), \end{aligned} \quad (\text{B4})$$

in agreement with Eq. (6.7). Note that the presence of the additional x^3 term (in $H^{(0)}$) in Eq. (B3) does not affect our leading-order estimate of δE_{LiVCS} . It can be shown that this term enters the perturbative correction at a higher order.

We extend the result here to the quadric case where

$$\begin{aligned} V_{\text{QD}} &= V_2 + V_4, \\ V_2 &= \frac{1}{2} m^* w_0^2 (x^2 + y^2), \quad V_4(x) = \frac{1}{4} k_{4x} m^* w_0^2 x^4. \end{aligned}$$

Asymmetry in the potential can be introduced by applying a dc gate voltage,

$$\begin{aligned} V &= V_{\text{QD}} + e\varepsilon_x^{(dc)} x \approx \frac{1}{2} m^* w_0^2 [(x - x_\varepsilon^{(dc)})^2 + y^2] \\ &\quad + \frac{1}{4} k_{4x} m^* w_0^2 (x - x_\varepsilon^{(dc)})^4 + k_{4x} m^* w_0^2 x_\varepsilon^{(dc)} (x - x_\varepsilon^{(dc)})^3, \\ &\quad \xrightarrow{x - x_\varepsilon^{(dc)} \rightarrow x} \end{aligned} \quad (\text{B5})$$

$$V = \frac{1}{2} m^* w_0^2 (x^2 + y^2) + \frac{1}{3} k_{3x} m^* w_0^2 x^3 + \frac{1}{4} k_{4x} m^* w_0^2 x^4,$$

$$k_{3x} = 3k_{4x} x_\varepsilon^{(dc)}, \quad x_\varepsilon^{(dc)} = -\frac{e\varepsilon_x^{(dc)}}{m^*w_0^2}.$$

Here we assume $\varepsilon_x^{(dc)}$ is weak [$e\varepsilon_x^{(dc)} \ll (m^*w_0^3)^{1/2}$ but $\varepsilon_x^{(dc)} \gg \varepsilon_x^{(ac)}$], and retain only the terms up to the order of $x_\varepsilon^{(dc)}$. Equation (B5) shows that the dc field produces a cubic term with the strength $k_{3x} = 3k_{4x} x_\varepsilon^{(dc)}$. Using the expression of δE_{LiVCS} derived earlier in the cubic case, we obtain

$$\begin{aligned} \delta E_{\text{LiVCS}} &= \tau_v \delta \mu_v^{(ac)} B_{\text{normal}}, \quad \delta \mu_v^{(ac)} = -\frac{3}{8} \mu_{v0} (k_{4x} x_\varepsilon^{(dc)} x_\varepsilon^{(ac)}) \\ &\quad \times \sin(w_{ac}t) \left(\frac{\hbar w_0}{\Delta} \right) \quad (\text{quadric case}), \end{aligned} \quad (\text{B6})$$

in agreement with Eq. (6.8). Note that the inclusion of the x^4 term in the potential in Eq. (B5) does not affect our leading-order estimate of δE_{LiVCS} . It can be shown that this term enters the perturbative correction at a higher order.

*yswu@ee.nthu.edu.tw

- ¹D. Deutsch, *Proc. R. Soc. London A* **400**, 97 (1985); P. W. Shor, in *Proceedings of the 35th Annual Symposium on Foundations of Computer Science*, edited by S. Goldwasser (IEEE Computer Society Press, Los Alamitos, CA, 1994), pp. 124–134; L. K. Grover, *Phys. Rev. Lett.* **79**, 325 (1997); M. A. Nielsen and I. L. Chuang, *Quantum Computation and Quantum Information* (Cambridge University Press, Cambridge, UK, 2000).
- ²K. S. Novoselov, A. K. Geim, S. V. Morozov, D. Jiang, Y. Zhang, S. V. Dubonos, I. V. Grigorieva, and A. A. Firsov, *Science* **306**, 666 (2004); A. K. Geim and K. S. Novoselov, *Nat. Mater.* **6**, 183 (2007).
- ³A. H. Castro Neto, F. Guinea, N. M. R. Peres, K. S. Novoselov, and A. K. Geim, *Rev. Mod. Phys.* **81**, 109 (2009).
- ⁴A. Rycerz, J. Tworzyclo, and C. W. J. Beenakker, *Nat. Phys.* **3**, 172 (2007).
- ⁵G. Y. Wu, N.-Y. Lue, and L. Chang, e-print arXiv:1104.0443.
- ⁶P. Recher, B. Trauzettel, A. Rycerz, Ya. M. Blanter, C. W. J. Beenakker, and A. F. Morpurgo, *Phys. Rev. B* **76**, 235404 (2007).
- ⁷A. Palyi and G. Burkard, *Phys. Rev. Lett.* **106**, 086801 (2011).
- ⁸D. Loss and D. P. DiVincenzo, *Phys. Rev. A* **57**, 120 (1998); G. Burkard, D. Loss, and D. P. DiVincenzo, *Phys. Rev. B* **59**, 2070 (1999).
- ⁹D. A. Lidar, I. L. Chuang, and K. B. Whaley, *Phys. Rev. Lett.* **81**, 2594 (1998).
- ¹⁰J. Levy, *Phys. Rev. Lett.* **89**, 147902 (2002).
- ¹¹M. Mohseni and D. A. Lidar, *Phys. Rev. Lett.* **94**, 040507 (2005).
- ¹²J. M. Taylor, H. A. Engel, W. Dur, A. Yacoby, C. M. Marcus, P. Zoller, and D. Lukin, *Nat. Phys.* **1**, 177 (2005).
- ¹³J. Petta, A. C. Johnson, J. M. Taylor, E. A. Laird, A. Yacoby, M. D. Lukin, C. M. Markus, M. P. Hanson, and A. C. Gossard, *Science* **309**, 2180 (2005).
- ¹⁴E. I. Rashba and A. L. Efros, *Phys. Rev. Lett.* **91**, 126405 (2003).
- ¹⁵V. N. Golovach, M. Borhani, and D. Loss, *Phys. Rev. B* **74**, 165319 (2006).
- ¹⁶C. Flindt, A. S. Sorensen, and K. Flensberg, *Phys. Rev. Lett.* **97**, 240501 (2006).
- ¹⁷B. Trauzettel, D. B. Bulaev, D. Loss, and G. Burkard, *Nat. Phys.* **3**, 192 (2007); P. Recher and B. Trauzettel, *Nanotechnology* **21**, 302001 (2010).
- ¹⁸H. Ingerslev Jørgensen, K. Grove-Rasmussen, K.-Y. Wang, A. M. Blackburn, K. Flensberg, P. E. Lindelof, and D. A. Williams, *Nat. Phys.* **4**, 536 (2008).
- ¹⁹A. V. Khaetskii and Y. V. Nazarov, *Phys. Rev. B* **61**, 12639 (2000).
- ²⁰D. V. Bulaev and D. Loss, *Phys. Rev. B* **71**, 205324 (2005).
- ²¹P. Stano and J. Fabian, *Phys. Rev. Lett.* **96**, 186602 (2006).
- ²²T. Meunier, I. T. Vink, L. H. Willems van Beveren, K.-J. Tielrooij, R. Hanson, F. H. L. Koppens, H. P. Tranitz, W. Wegscheider, L. P. Kouwenhoven, and L. M. K. Vandersypen, *Phys. Rev. Lett.* **98**, 126601 (2007).
- ²³A. Pfund, I. Shorubalko, K. Ensslin, and R. Leturcq, *Phys. Rev. B* **76**, 161308, (2007).
- ²⁴H.-A. Engel and D. Loss, *Phys. Rev. Lett.* **86**, 4648 (2001).
- ²⁵F. H. L. Koppens, C. Buizert, K. J. Tielrooij, I. T. Vink, K. C. Nowack, T. Meunier, L. P. Kouwenhoven, and L. M. K. Vandersypen, *Nature (London)* **442**, 766 (2006).
- ²⁶K. C. Nowack, F. H. L. Koppens, Yu. V. Nazarov, and L. M. K. Vandersypen, *Science* **318**, 1430 (2007).
- ²⁷S. Nadj-Perge, S. M. Frolov, E. P. A. M. Bakkers, and L. P. Kouwenhoven, *Nature (London)* **468**, 1084 (2010).
- ²⁸S. Y. Zhou, G.-H. Gweon, A. V. Fedorov, P. N. First, W. A. de Heer, D.-H. Lee, F. Guinea, A. H. Castro Neto, and A. Lanzara, *Nat. Mater.* **6**, 770 (2007).
- ²⁹G. Giovannetti, P. A. Khomyakov, G. Brocks, P. J. Kelly, and J. van den Brink, *Phys. Rev. B* **76**, 073103 (2007).
- ³⁰D. Xiao, W. Yao, and Q. Niu, *Phys. Rev. Lett.* **99**, 236809 (2007).
- ³¹The VOI in a graphene sheet is derived by P. Gosselin, A. Berard, H. Mohrbach, and S. Ghosh, *Eur. Phys. J. C* **59**, 883 (2009).
- ³²Also see P. Recher, J. Nilsson, G. Burkard, and B. Trauzettel, *Phys. Rev. B* **79**, 085407 (2009).
- ³³The impurity-caused intervalley scattering in a gapless graphene sheet is discussed by A. F. Morpurgo and F. Guinea, *Phys. Rev. Lett.* **97**, 196804 (2006).
- ³⁴J.-H. Chen, C. Jang, S. Xiao, M. Ishigami, M. S. Fuhrer, *Nature Nanotech.* **3**, 206 (2008).
- ³⁵M. Trif, V. N. Golovach, and D. Loss, *Phys. Rev. B* **77**, 045434 (2008).
- ³⁶J. J. Sakurai, *Advanced Quantum Mechanics* (Addison-Wesley, Boston, MA, 1967).